Seismic Studies in Support of Earth Source Heating at Cornell University: Stratigraphy in the Vicinity of ESH Candidate Drill Sites from Multichannel Seismic Reflection Profiling in 2018

Daniel May[1,2], Larry Brown[1], Olaf Gustafson[3] and Tasnuva Khan[1,4]

[1]Department of Earth and Atmospheric Sciences, Cornell University

[2] Now at Faculty of Civil Engineering and Geosciences, Delft University of Technology

[3] Cornell Facilities Engineering

[4] Now at Department of Geography and Geosciences, University of Erlangen-Nuremberg

Version 10-18-19

Note: Several figures in this report include data owned by Seismic Exchange, Inc. These figures have been modified to comply with the guidelines set forth by SEI.

Abstract

Multichannel seismic reflection surveys using vibroseis sources and nodal seismic recorders were carried out on and near Cornell University's Ithaca campus in support of the ongoing Earth Source Heat Project (ESH). These data were collected over a two-week period in September of 2018 with the help of student volunteers and subsequently processed to produce seismic reflection images of the subsurface near proposed geothermal drill sites. Although systematic noise from surface waves was found to be pervasive in the nodal recordings, basic stratigraphy in the immediate vicinity of the proposed well sites were delineated and identified with geological formations based on correlations with regional seismic surveys previously collected for gas exploration and available well data. Local structural disruptions in the dominant layer-cake stratigraphy at the target depths for geothermal drilling were found to be few and relatively minor in terms of offset geological units. These seismic images did not reveal any features that would preclude exploratory drilling for geothermal characterization at the drill sites under consideration.

Introduction

Developing a detailed understanding of geological stratigraphy and structure in the subsurface is a vital step in the planning of geothermal energy systems as their efficiency and safety is heavily dependent on rock permeability and connectivity within strata. The seismic reflection method is the geophysical technique that typically provides the highest resolution of geological features at depth, particularly for sedimentary basins, and is widely used as a primary guide in the drilling for oil and gas resources throughout the world (e.g. Waters, 1992). Here we report on a set of multichannel seismic reflection surveys (Figure 1) carried out in the immediate vicinity of two candidate sites under consideration for drilling as part of the Cornell Earth Source Heating Project. These surveys were designed to complement more distant, regional seismic reflection results previously collected for gas exploration and acquired as part of ESH planning. Although a portion of these industry surveys were also processed at Cornell (see companion report by T. Jordan), this report is focused on the surveys designed, acquired, and processed by Cornell staff and students.

The Cornell ESH surveys employed almost 400 ZLand GenII nodes (™ Fairfield Nodal , Figure 2) as receivers. These instruments were rented from SAExploration Services, (US) LLC, Stafford, Texas. The source used was a large (29,000lb) vibrator (T-Rex, Figure 2) rented from the NEES (Network for Earthquake Engineering Simulations) facility at the University of Texas at Austin. The nodal receivers were deployed primarily in linear subarrays along existing roads, although some were placed cross country. The source locations were restricted to accessible roadways (Figure 3).

Though the main objective of the seismic program was the collection of reflection data to aid decision making regarding the location of geothermal drill sites, the project also served as a means of community engagement. Perhaps the most direct way this engagement arose was through informal communication with residents while operating in the field regarding the purpose of the local seismic surveys, as well as discussion of the Earth Source Heat Project as a whole. In addition, engagement was fostered by the supplementary deployment of 5 earthquake type seismic stations on the Cornell campus and at the two nearest high schools, Ithaca High School and Dryden High school. In a spin-off study inspired by this engagement, some of the

nodes were deployed for a short period in a facility of the Cornell Veterinary School to monitor vibrations of interest in biological studies (May and Brown, 2019).

Field Operations

Seismic Reflection Profiling

The seismic reflection method is based on generating seismic waves that travel through the subsurface where they may be partially reflected by boundaries between rocks with different seismic properties and subsequently detected at the surface by motion detectors known as geophones (e.g. Reynolds, 2011). Reflection occurs when either the density or elastic constants of rock change. The time it takes for the seismic wave to leave the source and return to the surface after reflection, known as the two-way travel time, is proportional to the depth of the reflecting interface. Two-way travel time (TWT) can be converted to reflector depth if the speed of propagation- velocity- of the seismic waves through the intervening material is known. Seismic velocity can be measured *in situ* by using appropriate geometries for the seismic sources and receivers. The amplitude of the signal detected is related to the magnitude of the change in the seismic properties, or seismic impedance contrast. In the ESH surveys the seismic waves were generated by a truck known as a vibrator and detected by independently recording geophones, referred to here as nodes. These particular nodes were designed to measure only one component of ground motion, the vertical. The use of vibrating trucks as sources is often referred to as the vibroseis method. The receivers, or nodes, are often referred to as channels of recording.

Node Deployment

In the weeks prior to the arrival of the vibroseis truck, potential survey routes were identified by examination of satellite imagery (Google Maps) and direct inspection in the field. Preliminary receiver locations spaced 25 m apart were marked along the planned seismic lines and surveyed using a handheld GPS. These provisional locations were sent to SAExploration to be pre-programmed into portable computer terminals (YUMA) to facilitate nodal deployment. Unlike the typical wired receivers used in traditional seismic surveys, each of the nodes was a wireless instrument containing a battery and sensor enabling it to continuously record for extended periods of time (e.g. 3 weeks). The lack of cables between units allows for maximum flexibility in terms of where the units can be deployed. The drawback of independent recording devices is the inability to see the data recorded in real time while in the field.

Several student teams were tasked with the deployment of the instruments. The process required augering of holes approximately 8 inches in depth at each of the flagged receiver locations into which the nodes would be placed. In addition to serving as a security measure, burying the nodes minimized noise from wind and prevented them from being struck and/or losing coupling with the ground. The nodes were activated with small initiation units before being transported to the field and placed in the augered holes. Before the nodes were covered, the handheld terminals (YUMA tablets) were used to program the nodes with corresponding station numbers and locations as well as the selected sample interval of 2 ms. An additional parameter of note is the 10 Hz natural frequency of the nodes, which act as low-cut frequency filters. Once the nodes were programmed a Yuma tablet was again used to confirm that the node had established its GPS link for timing and that data acquisition was underway. After this initiation process was complete, the nodes were buried and continuously recorded data until they were harvested approximately three weeks later. The locations of the 382 nodes which were deployed

can be found in **Figure 1**. Along a few of the lines, cement bridges and private property prevented the deployment of nodes resulting in some gaps in receiver coverage.

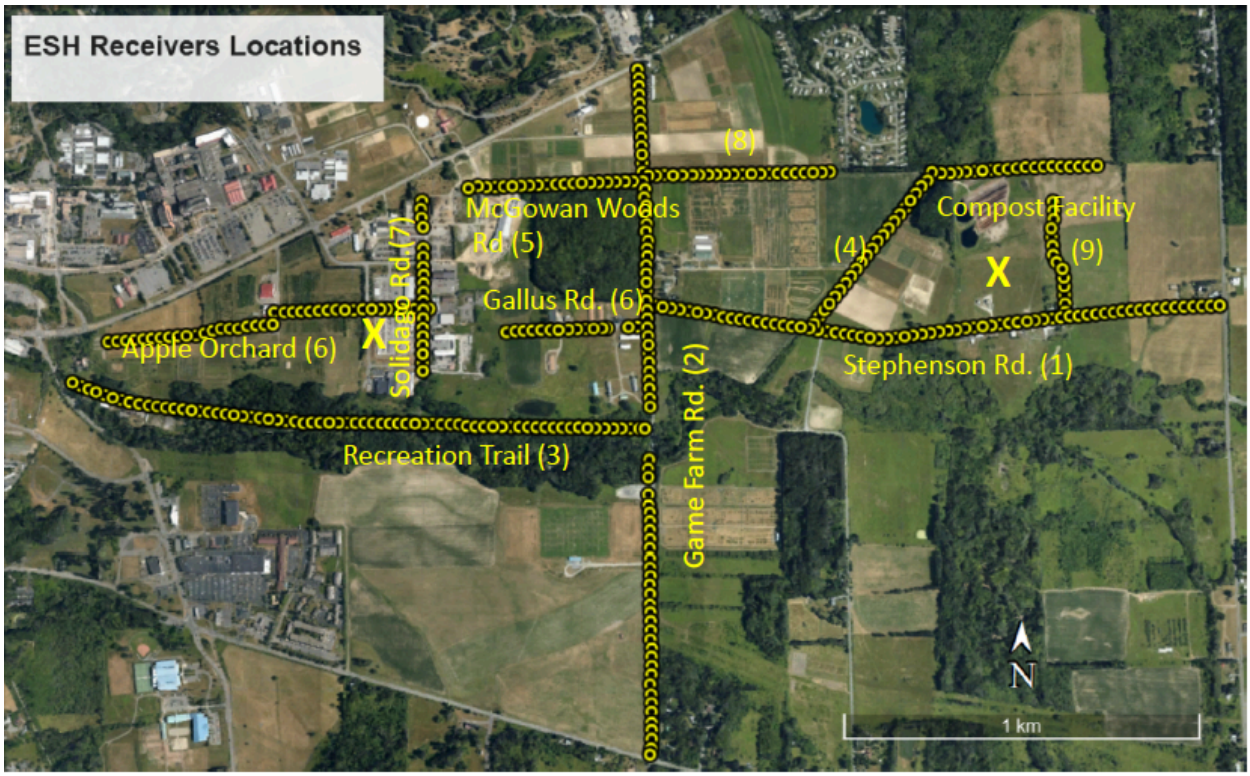

Figure 1: Locations of nodes (yellow dots) along the seismic lines to the east of Cornell's main campus. Potential drill sites near the Cornell Facilities on Solidago Road and the Cornell Composting Facility are marked with a yellow X.

Seismic Source

The seismic source, the NEES T-Rex vibrator (Figure 2), was operated by technicians from the University of Texas at Austin. T-Rex operations consisted of hydraulically lowering its vibrating pad, to which was attached a protective plywood sheet, to the ground then shaking the weight of the truck (29,000lbs) against the ground for 10-seconds while sweeping from frequencies of 5 to 80hz. These parameters were chosen to mimic those used by prior industry surveys in the area. The sweep interval was followed by a 20 second listening period before the next sweep. Multiple sweeps were made at each vibration station, or shot point, for later summation (vertical stacking) to enhance reflection signals and reduce noise.

Prior to production recording with the nodes, small test records were made of the vibroseis using a conventional 60-channel wired seismic recording system with geophone spacing of 4 m that was deployed alongside one stretch of nodes. This wired system allowed for collected data to be viewed in real time and was used to check the signal generated by the vibroseis truck. These test displays also helped inform the choice of acquisition parameters used in the production surveys

Figure 2: Left: Student volunteer placing nodal recorder into ground. Right: T-Rex, the vibroseis truck used for the ESH reflection surveys, delivers 10-second energy sweeps from 5-80 Hz.

During production operations, all the nodes deployed as shown in Figure 1 were continuously recording. However, the vibroseis was operated along only those segments of the nodal deployments which were accessible to the truck (Figure 3). The first segment, or line, surveyed was the East Ithaca Recreation Way, located to the south of the western proposed drill site (Figure 3). This survey began by recording 25 sweeps with vibroseis set to half power at each nodal position. However, vibrating along this line was terminated when it became apparent that the surface of the pathway was being weakened to the point that subsequent movement of the vibrator was damaging the pavement.

Although the majority of the remaining roads to be surveyed after this point were along paved roads designed to withstand normal vehicle traffic, as a precaution the number of sweeps per station was reduced to 10. Furthermore, in contrast to having all ten sweeps located at the same point on the ground, the vibrator was moved 2.5 m between sweeps, i.e. five sweeps on either side of the nodal station. These 10 records were subsequently summed (vertically stacked) during processing to represent a single source at that station location. This procedure was used for all shot points except along the lines within the Cornell Facilities and Cornell Orchards where only one sweep at half power was delivered at each station. This was due to the concern that excessive vibrating might cause damage to nearby buildings or underground utilities such as irrigation pipes. There are also gaps in vibration along several of the lines due to proximity to houses. Most notably, a large stretch towards the center of the Game Farm Road line was skipped to avoid disturbing nearby a raptor facility and botanical collections museum.

Upon completion of the vibrating, the nodes remained continuously recording in the field. Thus, in addition to capturing the Earth response generated by the vibroseis source, approximately two weeks of ambient vibrations were recorded. This passive data set has yet to be analyzed. At the end of the total recording period, the nodes were re-surveyed using a Trimble GPS in order to obtain more precise station positions. Finally, the nodes were uncovered, turned off using the handheld initiation unit, removed, cleaned, and returned to SAExploration for data harvesting.

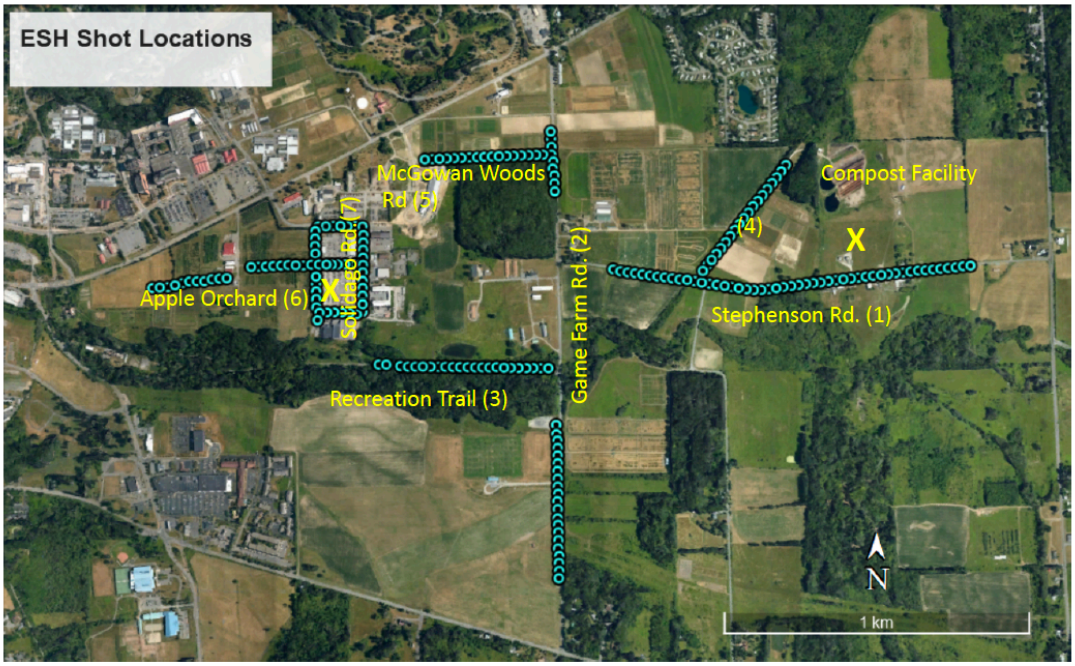

Figure 3: Locations of shot points (blue dots) along the seismic lines to the east of Cornell's main campus. Potential drill sites near the Cornell Facilities on Solidago Road and the Cornell Composting Facility are marked with a yellow X.

Earthquake Seismograph Stations

Five Sercel L-22 short period sensors on loan from the Incorporated Research Institutions for Seismology (IRIS) PASSCAL instrument facility were installed to monitor ground vibrations in the area around the vibroseis activity. The stations were intended to measure any vibroseis signals at larger distances, to detect any natural seismic activity in the area, but mostly to serve as a means of engaging the interest of the surrounding communities in the seismic work being carried out in support of ESH at Cornell. The L-22 has a natural (low-cut) frequency of 2 Hz and records three components of ground motion: vertical, north-south, and east-west. The sensors were connected to Reftek RT 130 Data Acquisition Systems (DAS) and GPS receivers (for timing control). The systems were powered by 12-volt car batteries that were kept charged either by 120V AC power supplies or solar panels. These instruments were placed on the Engineering Quad, next to the Cornell synchrotron, on the third floor of the East Campus Research Facility in the Cornell Veterinary School, and at both Dryden and Ithaca high schools. The L-22 sensors were buried approximately 6 inches below the surface to ensure good coupling with the ground, except for the instrument installed at the Vet School which was placed in a hallway isolated from major foot traffic. Data was recorded on two 2-GB memory disks which had to be swapped on an approximately monthly basis. Although these recordings are not part of this report, samples of earthquakes recorded by these instruments are shown in Appendix II. The deployment of the L-22 in the Vet School generated discussion of a more focused experiment to measure the buildings response vibrations, which is a concern to the operation of this facility. This led to deployment of spare nodes within the Research Facility. The results of those recordings are addressed in a separate report (May and Brown, 2019).

Data Processing

The continuous recordings provided to SAExploration were harvested in the form of 30 second-long “shot records” with time zero corresponding to the time of initiation of the vibroseis sweep. This time was determined by a recording system mounted directly upon T-Rex. These “raw” shot records were correlated with a synthetic 10-second, 5-80Hz sweep with a cosine taper to convert the extended vibroseis sweep into the more impulsive Klauder source wavelet for subsequent analysis (e.g. Waters , 1992). Next, the correlated shot records corresponding to the same shot location were summed, or vertically stacked, in order to produce a single, signal enhanced, seismic trace for each node position within a given shot gather. The stations used to define a specific shot gather correspond to conveniently defined segments of the nodal deployment in Figure 1. For example, processing illustrated in Figures 4-17 correspond to the nodes and shot points located along Stevenson Road (Figure 1, 3). The vibroseis correlation and all subsequent data processing was carried out using Schlumberger’s VISTA 2D-3D seismic processing software, a widely used tool in the oil and gas exploration industry.

After correlation, the coordinates and elevations of the effective source and receiver locations were added to the dataset, completing the preparation of the data for basic common midpoint (CMP) processing (e.g. Yilmaz, 1987).

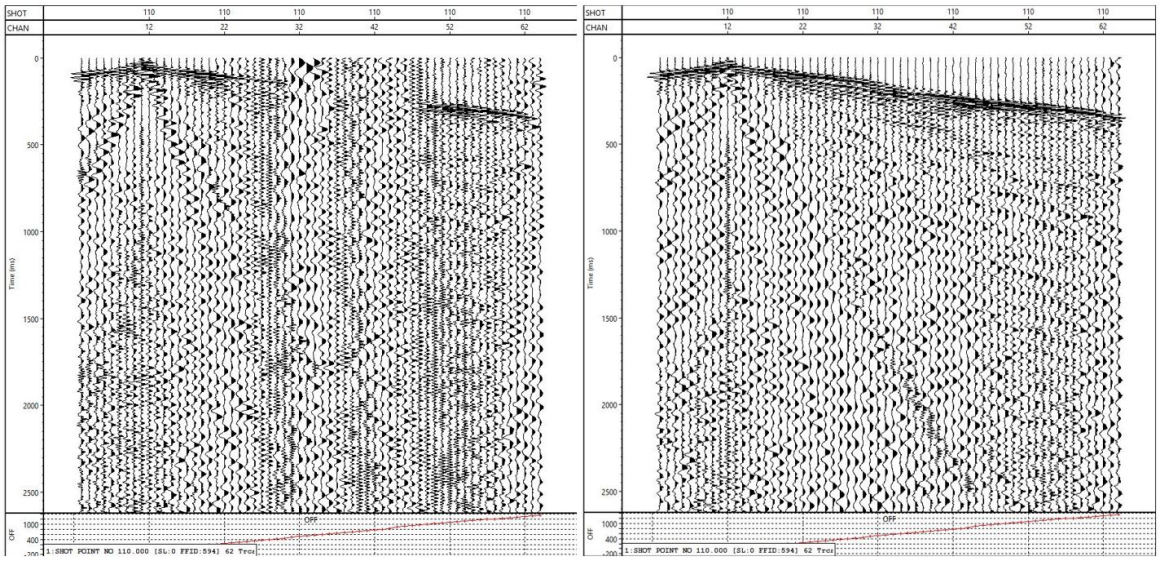

Figure 4: (Left) Vibroseis correlated record for one of ten individual shots that were summed to produce the vertically stacked shot gather for station 110 on Stevenson Road. (Right) Resulting stacked shot gather for station 110. Diversity stacking was used to reduce the influence of the noisy traces such as those seen in the unstacked record, while increasing the strength of any reflections. Recording was largely done along active roadways; traffic noise was persistent in the pre-stack records.

An early step in the data processing was to compensate for topographic variations among both shots and receiver locations. A fixed datum was selected to minimize this correction for each line, then time shifts due to elevation changes (elevation statics) were removed using the near surface velocities measured from first arrivals corresponding to the direct seismic wave

between shot points and nearby receivers. The final datum to which all lines were shifted after processing was 290 m above sea level, with a uniform replacement velocity of 3000 m/s.

After application of elevation statics, first-break picks for refracted arrivals (e.g. Yilmaz, 1983) were made on all the shot gathers along a line and then used to calculate of a model for spatial variations in near-surface velocities (**Figure 5**). This model was used to compute time shifts to apply to the data to compensate for relative time delays for seismic waves through near-surface heterogeneities that can degrade deeper imagery. The shallow velocity model created for Stevenson Road can be seen in **Figure 5**. Note, that such refraction models were only created for profiles where both receivers and shots were located along the same line (i.e., Lines 1-7). Refraction models generated from data where receivers and shots were located on parallel, but offset lines, were deemed inaccurate due to lack of near-offsets to define shallow velocity variations and the violation of the assumption of 2-D geometry inherent in the refraction analysis software tool.

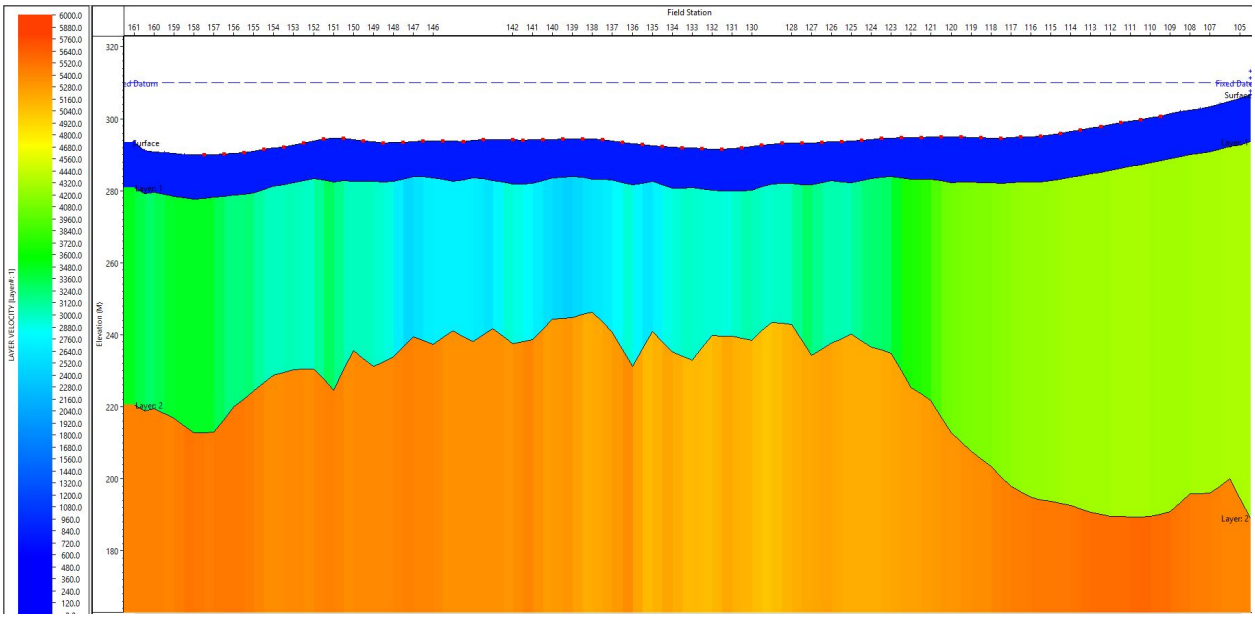

Figure 5: Shallow velocity model (west to east) along the Stevenson Road line calculated from first-break picks. Velocities and elevations are in m/s and meters, respectively. A weathering layer, shown in blue, of 800 m/s was assumed.

Figure 6 illustrates the primary challenge for data processing, the presence of very strong surface waves which obscure reflections at larger offsets and depths. These slow-moving waves are ubiquitous and largely unaffected by vertical stacking. They tend to be more problematic at shorter offsets, i.e. for receivers located closer to the energy source. They were especially problematic in the ESH surveys because the roads available for deployment were relatively short, thus limiting the available range of source to receiver offsets. Another contributing factor was the use of single geophones (nodes) for recording. Conventional wired recording systems typically employ multiple sensors at each receiver location deployed in a spatial array designed to reject surface waves before recording. Such arrays are usually not practical with nodal deployments, and the task of surface wave rejection is left to subsequent data processing. In this case, several processing techniques were employed in an attempt to remove the surface waves

and correspondingly enhance any underlying reflection energy. These included Ormsby frequency band-pass filtering, frequency-wavenumber (F-K) filtering, trace averaging, or some combination thereof. The effectiveness of such processing is illustrated by the examples in **Figure 6**.

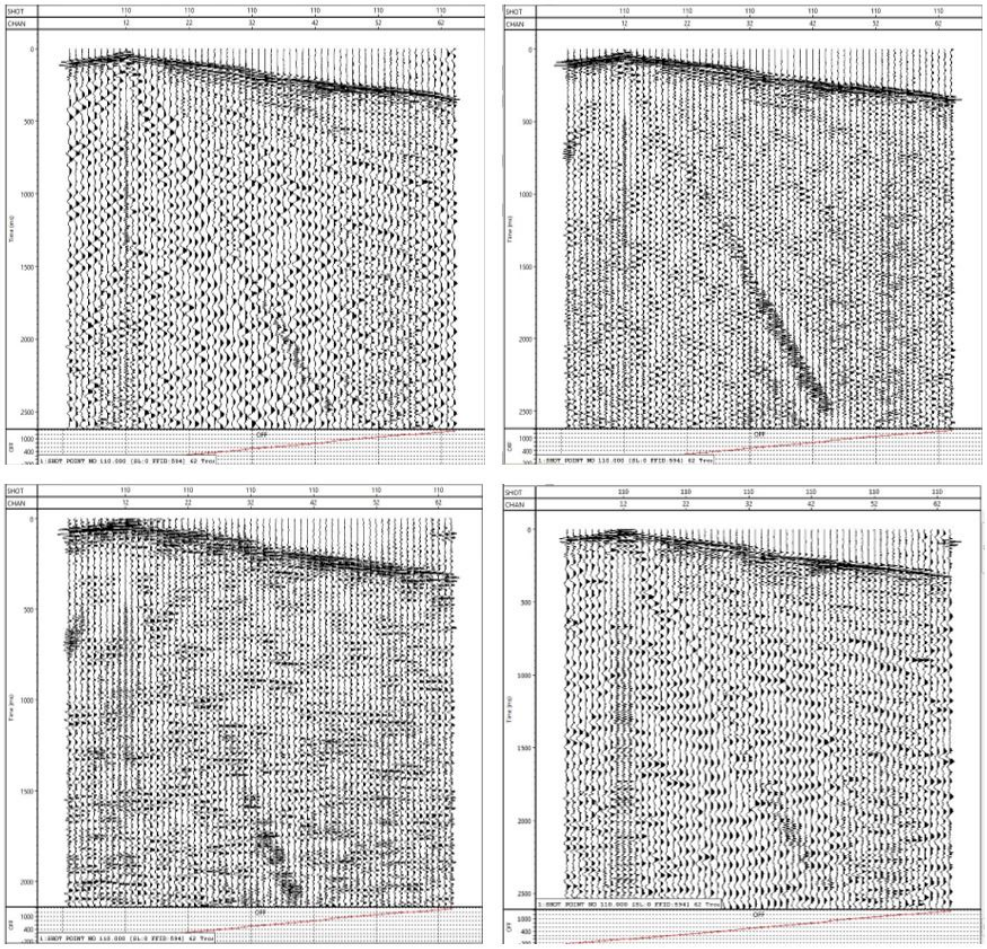

Figure 6: Top left: A representative correlated shot gather after vertical stacking, dominated by surface wave energy. Top right: same shot gather after application of low cut frequency filter. Lower right: shot gather after application of F-K filter designed to reject slowly propagating energy. Lower right: shot gather after applying a 3-trace running average filter.

A simple a low-cut band-pass filter reduces much of the surface wave energy in the near offset traces but does not reveal much in the way of underlying reflection energy. F-K filtering also significantly reduces the amount of surface energy at the near offsets. However, such filters tend to generate artifacts in the form of sub-horizontal linear energy which obscure true reflections with similar travel time patterns. The 3-trace running averages mimic the common industry practice with traditional wired systems of adding the response of multiple receivers to form a receiver array that acts as a spatial filter before recording. Although the running average appears to have enhanced already visible reflections, it did little to remove the surface wave energy. Using a larger number of traces in the running average is more effective at cancelling surface wave noise, but risks degrading shallow reflection signals which are not linear with

offset. Ultimately, a combination of low-cut band-pass filtering and deconvolution to enhance higher frequencies followed by a 3-trace running average was found to be the most effective treatment of the shot gathers.

Subsequent processing (**Figure 7**) varied slightly among the surveyed lines, but generally consisted of a conventional sequence associated with common depth point stacking to produce a seismic reflection image (Yilmaz, 1987)

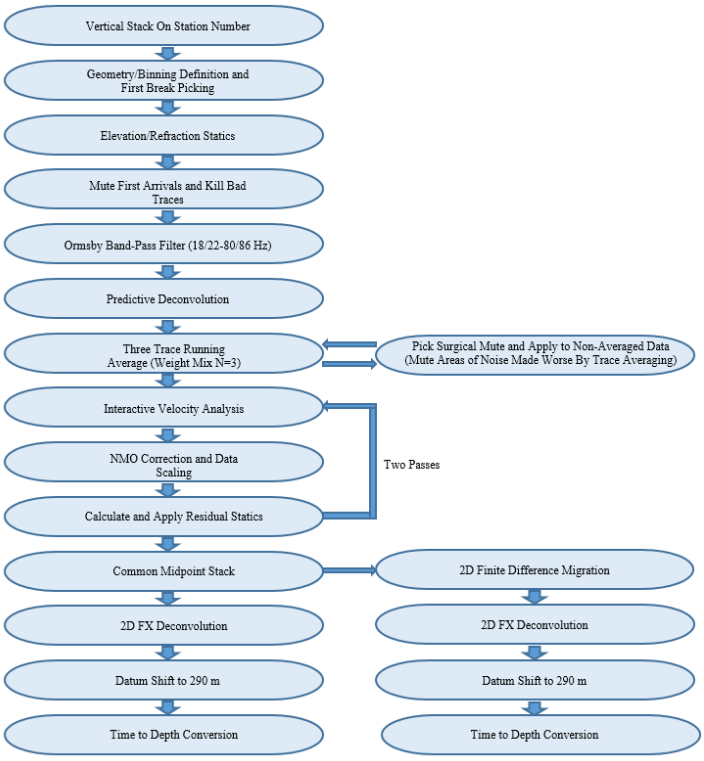

Figure 7: General processing flow used to produce seismic time and depth sections. Slight variations to this flow were made during the processing of certain lines, often in the form of additional surgical mutes applied to the data.

Once elevation and refraction statics were calculated and applied to each of the lines and measures were taken to remove surface wave energy, top mutes were applied to remove the direct and refraction arrivals, and obviously bad traces were visually edited from the records. Additionally, surgical mutes were used to remove portions of data where the surface waves or the sound waves (air wave) were particularly resistant to filtering. The data also underwent predictive deconvolution to enhance the high frequency content of reflections, with whitening varying from 5-10% depending on which value most improved the visibility of reflections. After this preparatory work, the data were sorted into common midpoint (CMP) bins as a prelude to the velocity analysis and normal moveout corrections that are key to signal enhancement by CMP stacking (Yilmaz, 1983). CMP processing is based on the assumption that, for sufficiently flat layers, the recorded seismic traces that correspond to shot locations and receiver locations that share a common midpoint are redundantly recording reflection energy form the same subsurface points. Correcting the travel times for the different source-receiver offsets associated with traces that share a midpoint (e.g. CMP gather) allows these redundant signals to be added constructively while simultaneously destructively adding noise components. These Normal Moveout (NMO) corrections require estimates of subsurface velocity which can be derived from

the reflection records themselves (See below). Since the source and receiver lines are not perfectly straight, the midpoints between a shot and receiver do not in general lie directly beneath either. The final CMP stacked images correspond to the position of the CMP positions defined by the binning process mentioned previously. The CMP locations that correspond to the stacked sections reported here are shown in **Figure 8**.

Figure 8: Common midpoint positions defined by the ESH surveys, with the location of the seismic image associated with the Stevenson Road survey marked in green. Potential drill sites near the Cornell Facilities on Solidago Road and the Cornell Composting Facility are marked with an X.

An initial velocity analysis was conducted using standard tools available in VISTA. These tools are all based upon fitting a theoretical hyperbolic travel time curve (e.g. travel time vs source receiver offset) corresponding to a trial velocity to the observed travel times of reflected energy in the CMP gathers. The resulting velocity estimates were checked for reasonableness by comparison to the relatively few *in situ* measurements available from local well logs. An example of velocity picking for one subset of common midpoint gathers is shown in **Figure 9**. Velocity files for each of the processed lines can be found in the supplemental materials accompanying this report.

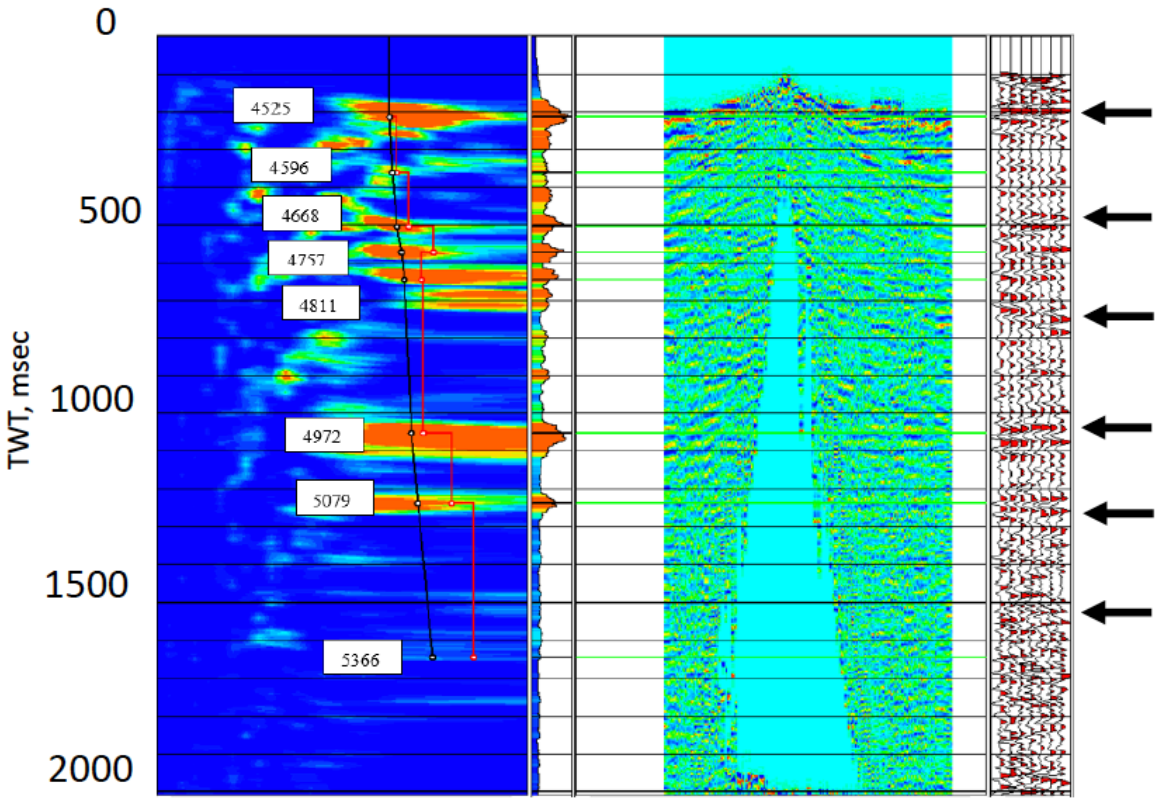

Figure 9: Velocity analysis for a selected subset of common midpoint gathers from the Stevenson Road Line. Left: Velocity analysis by computing semblance between traces in the summed CMP gathers (super-gather) after NMO corrections for a suite of trial velocities. High semblance implies travel time alignment of reflection energy by the NMO corrections associated with a given trial velocity. Visual picks of the optimal stacking velocity as represented by the semblance maxima are indicated by the numeric displays and black line. The associated interval velocities computed using the Dix equation are indicated by the red line. Center: The corresponding CMP gather with the NMO corrections corresponding to the velocity vs depth curve picked on the semblance display applied. Reflections should appear as horizontal alignments of energy (e.g. black arrows) Right: A seismic section corresponding to the CMP gather subset computed using these velocity picks.

From the initial velocity analysis, an initial, or brute, stack was generated. The brute stack was used as a model to fine tune the alignment of reflections within CMP gathers by the computation of residual statics. Residual statics are time shifts calculated from cross correlating seismic traces within a CMP gather with the corresponding stacked trace in the brute stack. These residual statics were then applied to the CMP gathers without an NMO correction and velocity analysis was repeated. After the third iteration of this process, a final set of residual statics were calculated. These statics were applied to the NMO corrected gathers which were subsequently stacked to create the final time section. In order to enhance amplitude of linear energy in the stacked section, which we interpret to be primarily due to reflections, a coherency enhancement procedure known as FX deconvolution was applied. The stacked section for Stevenson Road both before and after FX deconvolution is shown **Figure 10**.

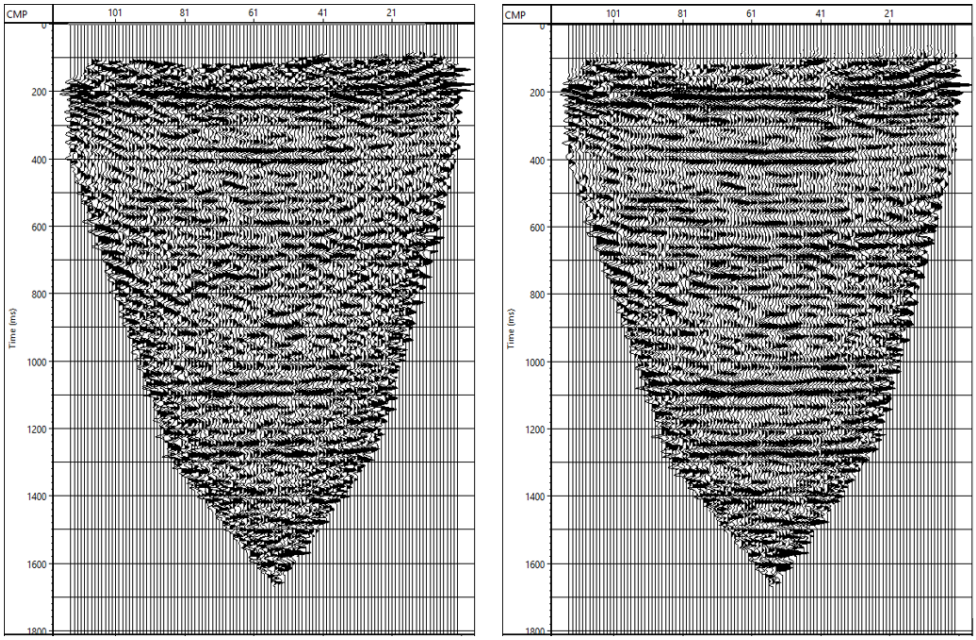

Figure 10: Final time section for the Stevenson Road line both before (left) and after (right) FX deconvolution. The vertical axis is in milliseconds and represents two-way travel time. The horizontal axis is labelled with the CMP bin number. The CMP bins are spaced 12.5m apart. The shape of the base of this image is due to muting of surface wave domination of the image at depth, which is a function of distance from the end of the survey.

Post Stack Processing

Using the velocity models generated for each of the profiles, a post stack finite difference time migration was applied in order to relocate dipping energy to its proper positions in the subsurface (Yilmaz, 1987). The input to the migration flow was the final stack without FX deconvolution, with FX deconvolution reapplied after migration. The result of the migration of the Stevenson Road seismic image is shown in **Figure 11**.

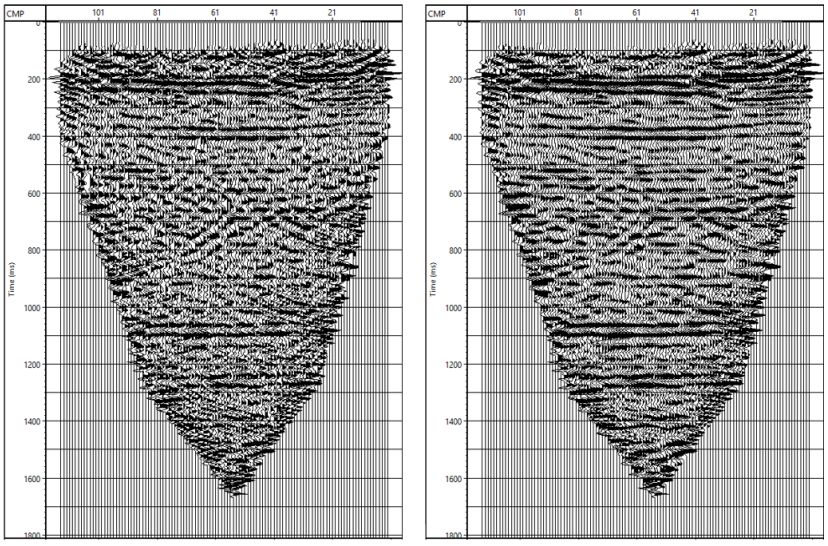

Figure 11: Migrated time sections for the Stevenson Road line. The profile is shown both before (left) and after (right) FX deconvolution. The vertical axis is in milliseconds and represents two-way travel time. The horizontal axis is labelled with the CMP bin number. CMP bins are spaced 12.5m apart.

Finally, an appropriate spatially varying but smoothed velocity model was developed from the CMP velocity analyses and used to convert travel time to depth **Figure 12**.

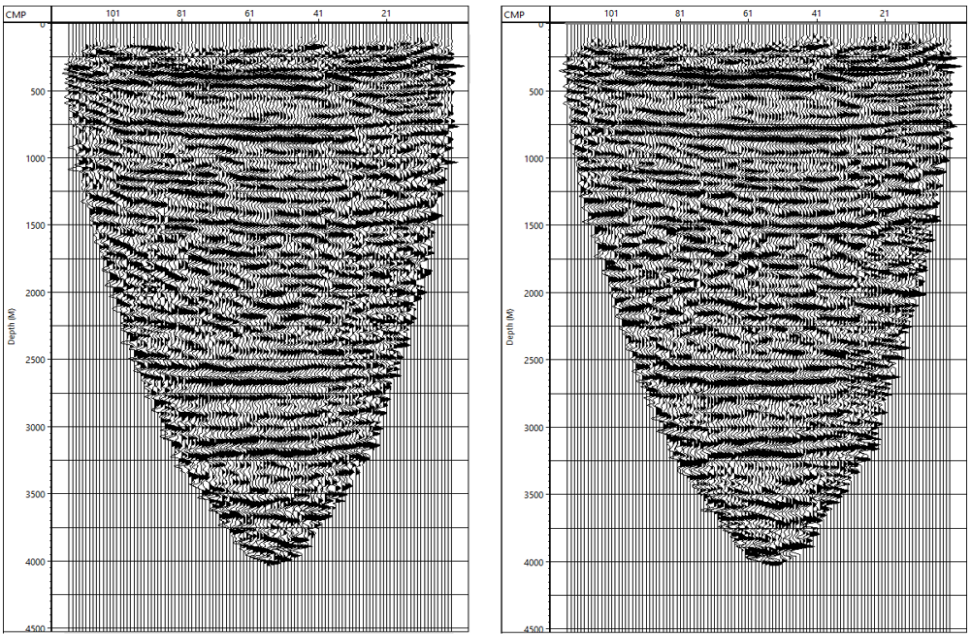

Figure 12: Depth sections for the Stevenson Road line. The depth conversion has been applied to the unmigrated (left) and migrated (right) time sections after application of FX deconvolution. The vertical axis is depth in meters. The horizontal axis is labelled with the CMP bin numbers. CMP bins are spaced 12.5m apart.

Midpoint maps, shallow velocity models computed from refraction analysis, and similarly computed seismic time and depth sections for the other primary lines in the survey are shown in **Appendix I** and cited as appropriate in the following discussion of the data.

Data Interpretation

Regional Context

Conclusive interpretation of the reflections mapped by the ESH seismic reflection sections near the proposed drill sites will require calibration against future well data. However, a reasonable basic interpretation can be derived by comparison of the reflection character apparent on the ESH seismic sections with that seen on relatively nearby seismic reflection sections collected by the oil and gas industry which have been constrained by well data. Since these industry lines were collected with different equipment and significantly different acquisition parameters (most notably aperture, or the maximum source receiver offset available) the character of the two different datasets should not be expected to match in detail. However, the reflection character of various geological strata appears to be sufficiently distinct to make convincing correlations between the two types of images. Two small portions of stacked seismic sections of data purchased from Seismic Exchange Inc., and processed by Star Geophysics Inc., are shown in **Figure 13**. The stratigraphic identifications shown in Figure 13 are by Prof. Teresa Jordan at Cornell University based upon her integration of the seismic data with available well data in the area. To avoid depth ambiguities related to possible errors in velocity estimations

among the various datasets, the correlations discussed below are based on comparison of time rather than depth sections.

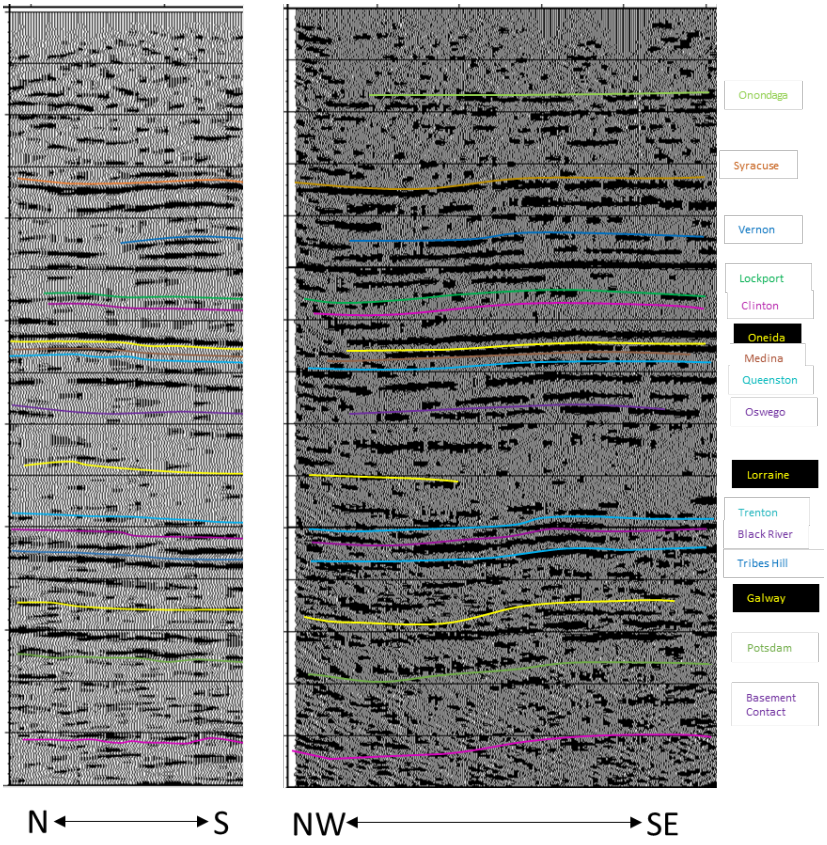

Figure 13: Industry seismic sections collected near the eastern limit of the Cornell vibroseis surveys. These data were collected in 2007 for oil and gas exploration and are owned or controlled by Seismic Exchange, Inc. The data are leased by Cornell University and processed by Star Geophysics. The stratigraphic interpretation is provided by Professor Teresa Jordan. Horizontal axis represents distance. Vertical axis represents two-way travel time.

Strong reflectivity at depths less than 500 m, which correspond to Silurian formations such as the Salina, show evidence of disruption by folding and or faulting that we interpret to represent salt tectonics that appears to be decoupled from any deformation below. Of more relevance to ESH drilling are the underlying Paleozoic formations. A zone of weak reflectivity is evident below the Queenston Formation followed by a pair of reflectors straddling the top of the Tribes Hill formation. Further down, another pair of strong reflectors are interpreted to be a horizon within the Galway Formation and the contact between the Galway and Potsdam formations, respectively. Below the Potsdam, faint signs of the contact between sedimentary strata and basement rock can be seen. These features of the industry surveys, along with some background knowledge of the local geology, are the basis of formation identification on the ESH seismic sections.

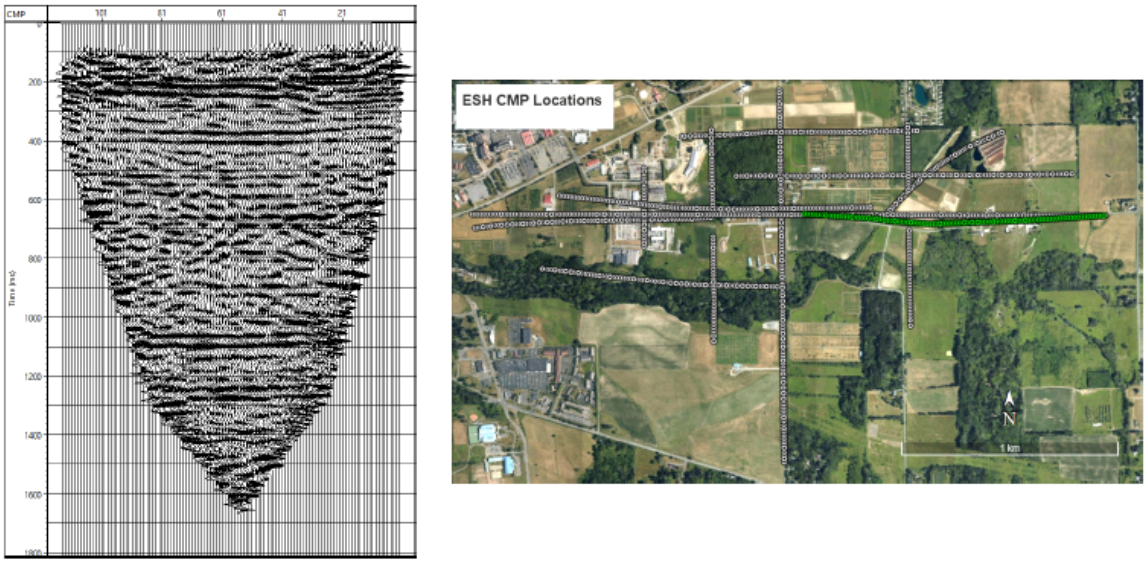

Figure 14: Left: Line 1 (Stevenson Road) seismic time section after migration and FX deconvolution. Oriented from west (left) to dast (right). Vertical axis represents two-way travel time in sec. The horizontal axis is labelled with the CMP locations which are spaced 12.5m apart. Right: Location of the CMP line (shown in red. .

Line 1 (Stevenson Road)

A zone of low reflectivity between 650 and 1050 ms TWT on the seismic time section for Line 1 (Stevenson Road) correlates with the similarly non-reflection gap between the Queenston and Tribes Hill identified on the industry profile as well as being consistent with the expected depth of these formations based upon regional geological projections. The two strong reflections at approximately 1060 ms and 1100 ms likewise seem to correspond to reflections of similar intensity on the industry line which represent the boundary between the Black River and Tribes Hill formations. The prominent reflection at about 1290 ms correlates well with what is interpreted to be the top of the Potsdam Formation on the industry data. The reflection at approximately 1430 ms is a reasonable choice for the contact between the Potsdam formation underlying Pre-Cambrian metamorphic basement. This interpretation suggests a westward dip of the strata when compared to the industry profile. A summary of these identifications and their correlation to industry data is shown **Figure 15**.

Line 1/5 (Stevenson Parallel)

Using the recordings of receivers along Line 5 (McGowan Woods Road) of shots on Line 1 (Stevenson Road) and vice versa, a CMP profile running parallel to Stevenson Road through the Compost Facility was generated (**Figure 16)**. Due to the large minimum offsets between sources and receives for this geometry, contamination of the data by surface waves is reduced. However, this lack of near offset recordings results in loss of energy from reflectors at greater depths.

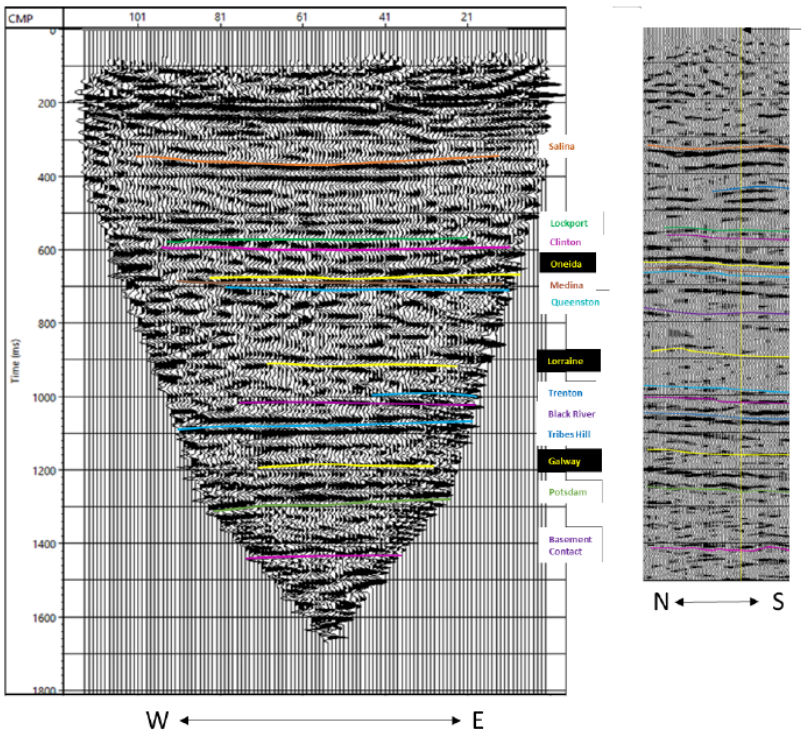

Figure 15: Left: Line 2 (Stevenson Road) seismic time section after migration and FX deconvolution. Right: Interpretation of matching strong reflectors on an industry profile at a projected point of intersection. Of particular note, the two strongest reflectors in the region between 1060 and 1100 ms on the Cornell line are taken to represent the same two strong reflectors straddling the blue line on the industry profile marking the Tribes Hill. The vertical yellow line on the industry data here and subsequent figures marks the position of intersection or projected intersection with the Cornell vibroseis line to the left.

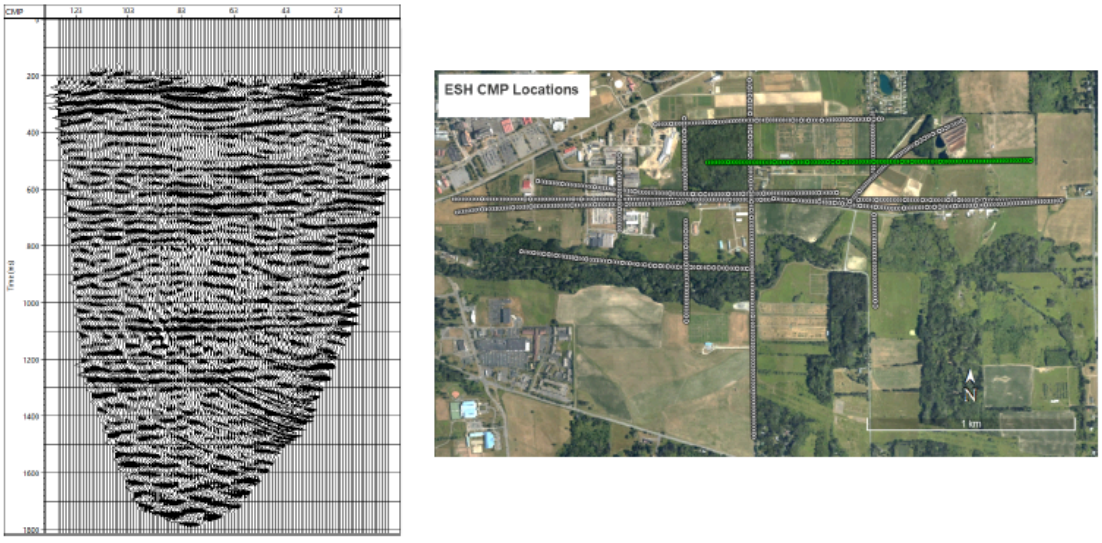

Figure 16: Left: Seismic time section for Line 1/5 (Parallel to Stephenson Road), oriented west to east. The seismic section has been migrated and FX deconvolution applied. Vertical axis is two-way travel time. in milliseconds. The horizontal axis is labelled with the CMP bin numbers. CMP bins are spaced 12.5m apart. Right: Location of CMP line (shown in red).

The relative lack of surface wave energy has resulted in a much clearer image of the deeper stratigraphy. Two distinct reflectors at approximately 1050 and 1090 ms beneath a zone of relatively low reflectivity are again interpreted as the boundary between the Black River and Tribes Hill Formations **(Figure 17).** The strong reflection at approximately 1280 ms is interpreted to be the top of the Potsdam. These reflections match well to similar events on the Stevenson Road profile (Line 1). However, a distinct reflector that would reasonably correspond to the top of crystalline basement is not present on this section. The two short reflections between 1500 and 1600 ms, appear to be too deep for top of basement, but could correspond to intra-basement heterogeneity.

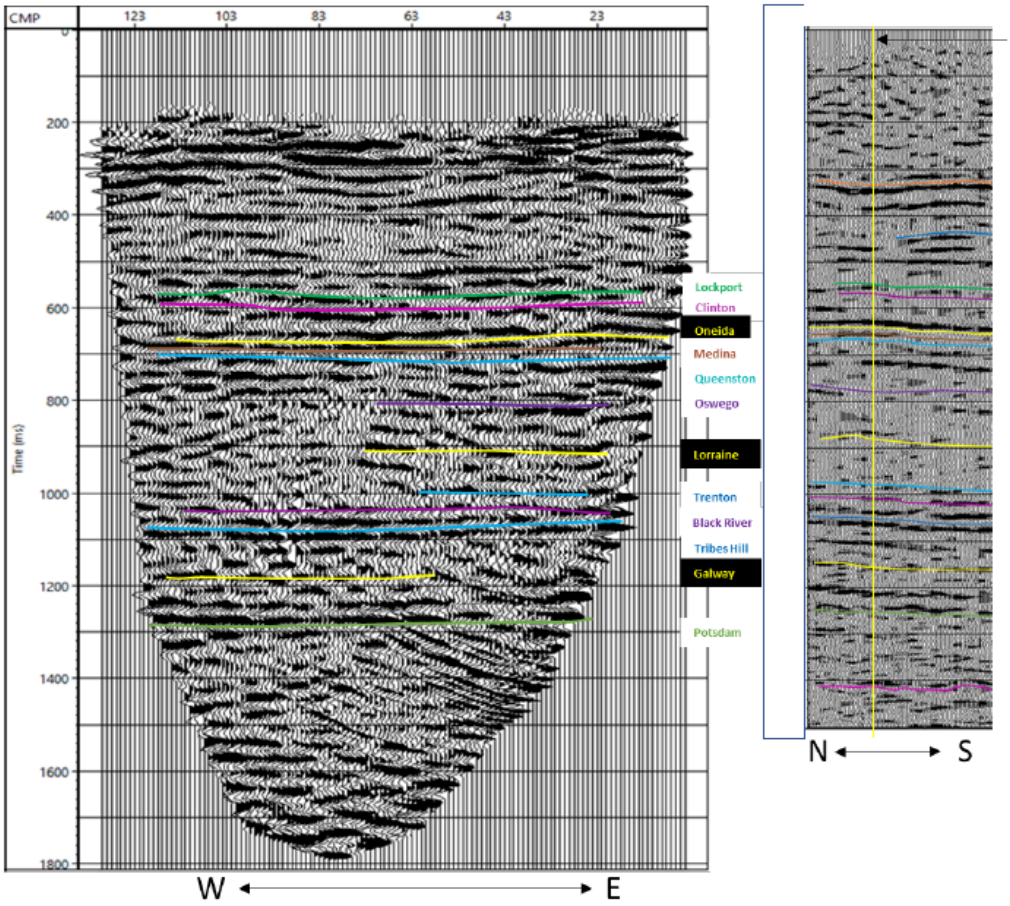

Figure 17: Left: Line 1/5 (Parallel to Stevenson Road) parallel seismic time section after migration and FX deconvolution. Right: Industry seismic section. Interpretations is based on correlation of reflections as shown by colored lines.

Line 5 (McGowan Woods Road)

A third reflection profile, parallel to the two previously discussed, is located along McGowan Woods Road **(Figure 18)**. One noteworthy aspect of this line is that the number of shot points (17) was far fewer than on Stevenson Road (49), resulting in a lower CMP stacking fold. However, this road was used as a demonstration area for the vibroseis truck so additional sweeps are available. Because McGowan Woods road is unpaved, a stronger vibroseis sweep was also used.

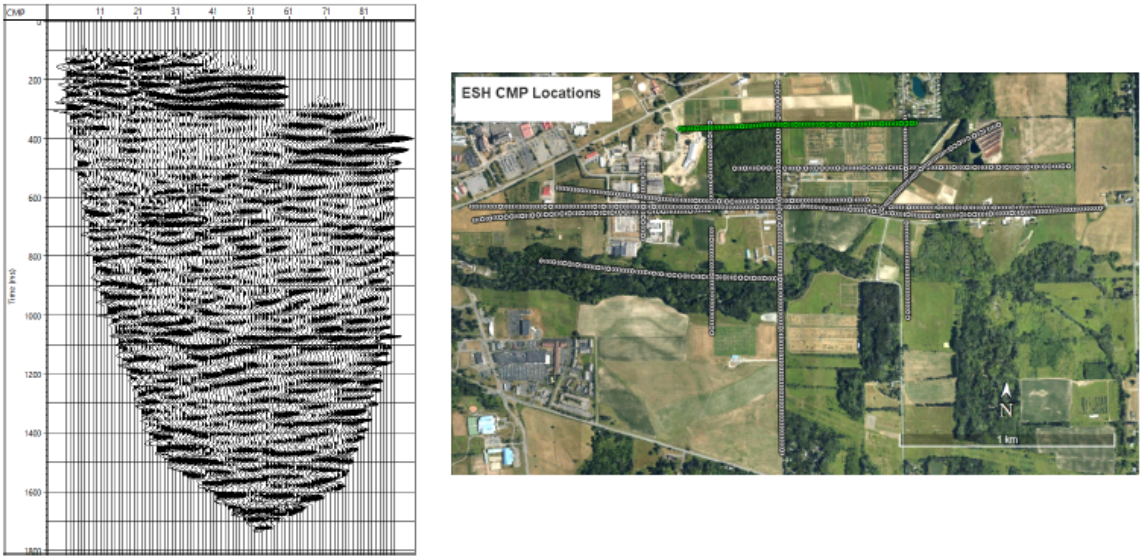

Figure 18: Left: Line 5 (McGowan Woods Road) seismic time section after migration and FX deconvolution, oriented West-East. Vertical axis of seismic section is two-way travel time in milliseconds. The horizontal axis is labelled with CMP bin numbers. CMP bins are spaced 12.5m apart. Right: Location of CMP line (shown in red).

Although the western portion of the time section loses some coherency, there are fairly strong reflections at 1040 and 1080 ms, here interpreted to be the boundary between the Black River and Tribes Hill Formations, and at 1260, interpreted to be the top of the Potsdam (**Figure 19**). Reflections at 1370 ms or 1450 ms are candidates for the contact between the Potsdam and the basement. Unlike in the previous two-way time sections, the Tribes Hill is not placed between the two strongest reflections. This interpretation is based on the assumptions that the difference in travel times between this line and the nearby industry line should be similar for both the Potsdam and Tribes Hill. Furthermore, the northern section of the industry line in **Figure 19** shows an additional strong reflection below the pair which surrounds the Black River and Tribes Hill contact.

Line 3/5 (Parallel to Recreation Trail)

Using the recordings from receivers along Line 5 (McGowan Woods Rd) of shots on Line 3 (Recreation Trail) and vice versa, a CMP profile that passes directly through the westernmost candidate drill site was generated (**Figure 20)**.

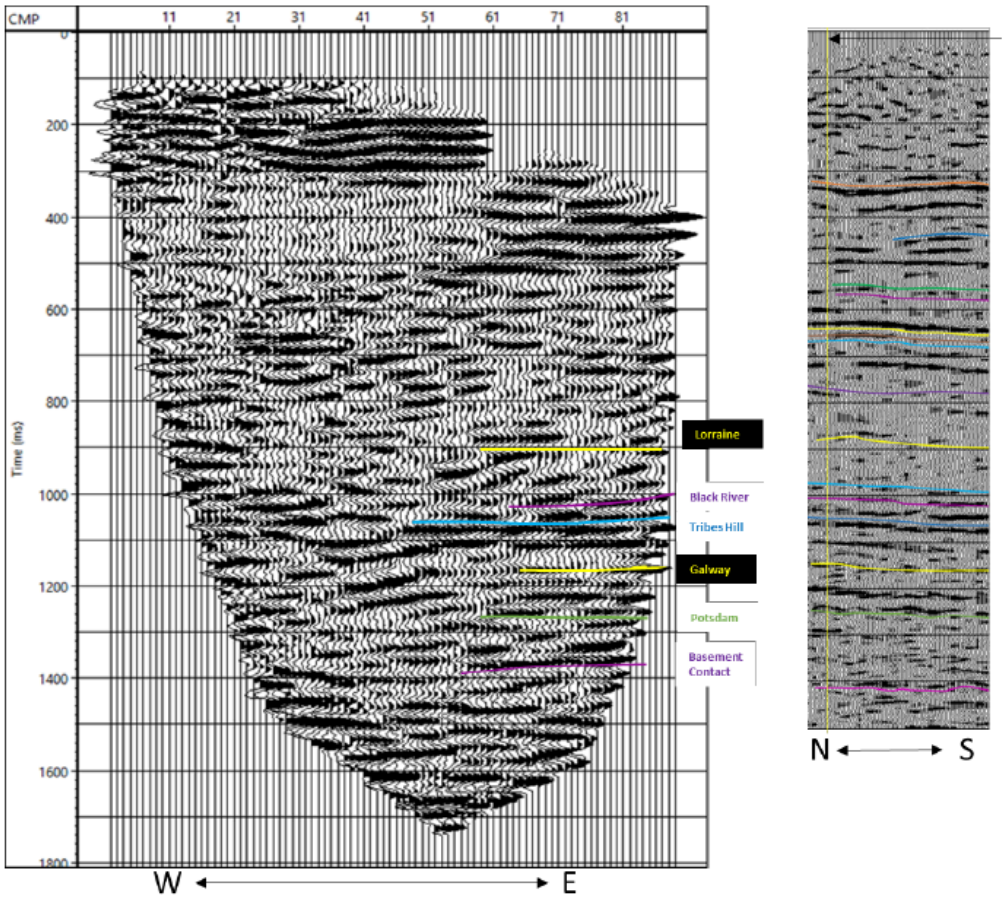

Figure 19: Left: Line 5 (McGowan Woods Road) seismic time section after migration and FX deconvolution. Right: Industry profile at a projected point of intersection of the two lines. The strong reflectors at 1040 and 1080 ms are interpreted to be the two strong reflectors straddling the blue line that mark the Tribes Hill Formation.

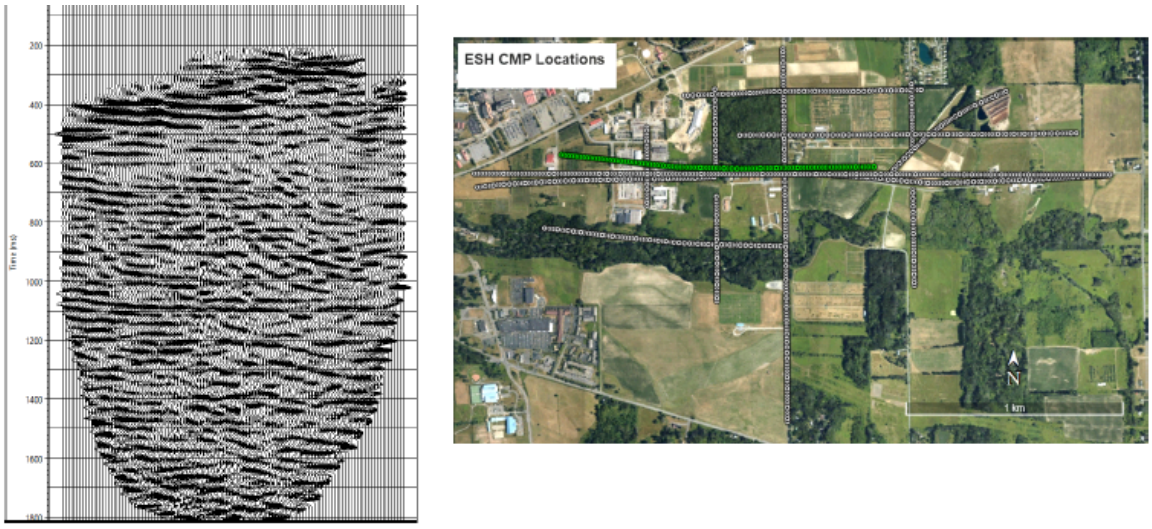

Figure 20: Left: Line 3/5 (Parallel to Recreation Trail) seismic time section after migration and FX deconvolution. Oriented west (left) to east (right). Vertical axis of seismic section is two-way travel time in milliseconds. The horizontal axis is labelled with the CMP bin numbers. CMP bins are spaced 12.5m apart. Right: Location of \CMP line (shown in red).

Reflections on this section are not as clear as those on the Line 1/5 (Parallel to Stevenson road) despite the similar shot and receiver geometry. This may be the result of the use of lower power sweeps on the recreation trail. Nevertheless, it is possible to identify some of the prominent reflections which have been identified on other lines. The most noticeable and continuous of these can be seen at 1060 and 1100 ms, which we interpret as the boundary between the Black River and Tribes Hill formations (**Figure 21**). The top of the Potsdam is not very distinct; discontinuous reflections around 1270 ms are plausible candidates. Eastward dipping energy at the eastern end of the line is an artifact of low stacking fold and migration edge effects.

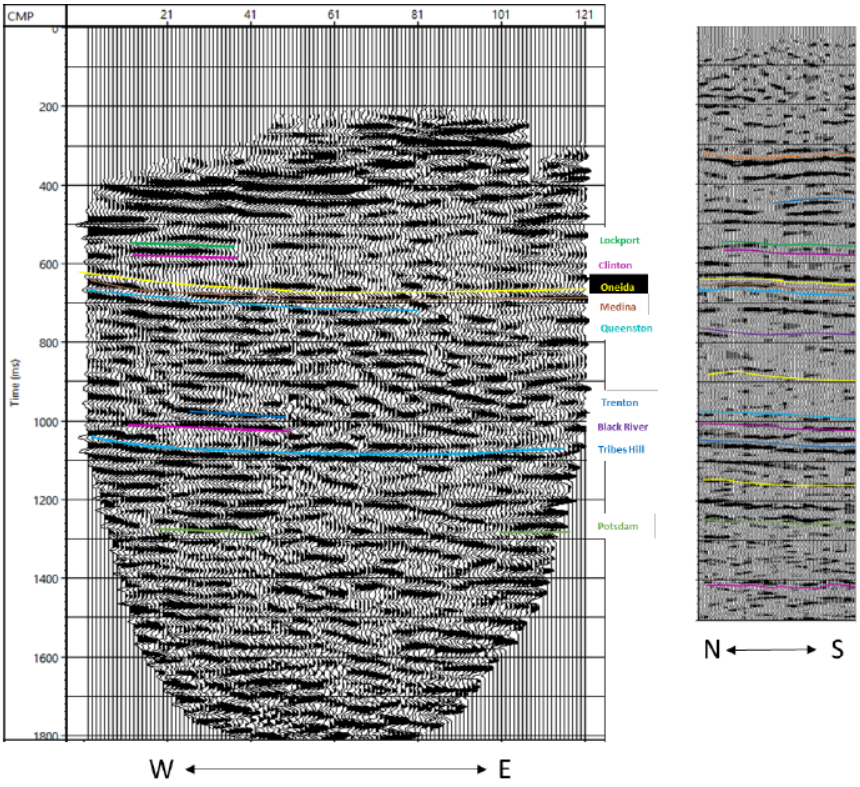

Figure 21: Left: Line 3/5 (Parallel to Recreation Trail) time section after migration and FX deconvolution. Right: Industry seismic line near but not intersecting line 3/5. The two strongest reflectors, between 1060 and 1100 ms, is interpreted as the boundary between the Black River and Tribes Hill Formations

Line 1/3/5/6 (Stevenson Road/Facilities)

In order to take advantage of the data redundancy towards the center of the receiver deployment, shots and receivers from lines 1,3,5, and 6- all running west to east-were processed to create one seismic section. This essentially re-images the lines along Stevenson Road and parallel to the Recreation Trail but with a larger stacking fold by including shots from line 6. The time section and corresponding CMP locations are shown in **Figure 22**.

The increased stacking fold seems to have resulted in more distinct reflections beneath the eastern portion of the line. Reflections between 1060 and 1100 ms are again interpreted as the top of the Tribes Hill Formation (**Figure 23**). Reflection continuity is much poorer beneath the western portion of this line, perhaps due to the greater contamination of surface wave energy

at the offsets that correspond to this portion of the line. Despite this reduction in continuity, a reflector corresponding the Tribes Hill Formation can be identified, exhibiting the eastward dip present on Line 3/5 (parallel to the Recreation Trail).

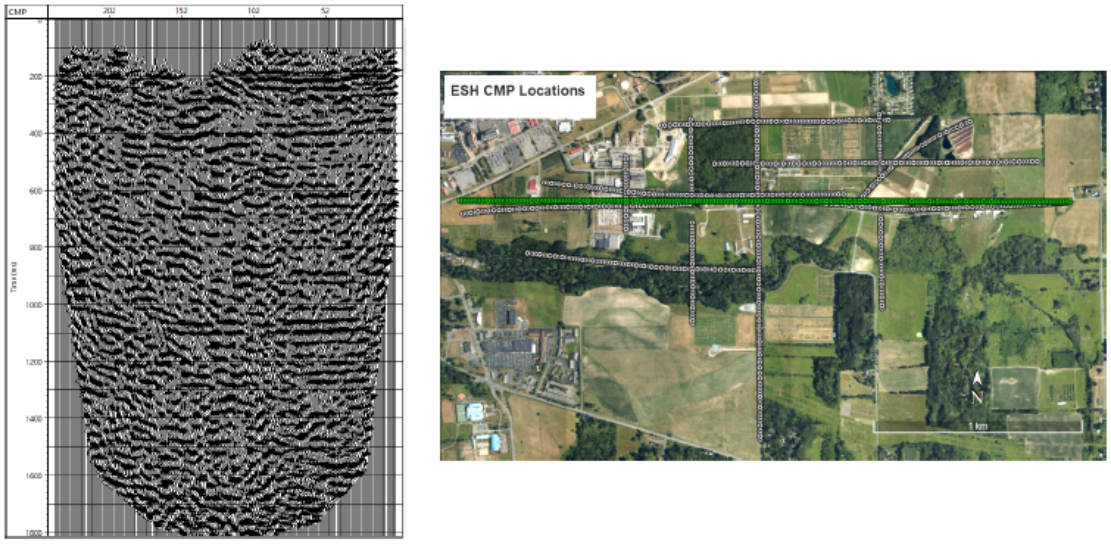

Figure 22: Left: Line 1/3/5/6 (Stevenson/Facilities) seismic time section after migration and FX deconvolution. Orientation is from west (left) to east (right). Vertical axis is two-way travel time. The horizontal axis is labelled with the CMP bin numbers. CMP bins are spaced 12.5m apart. Right: :Location of CMP line (shown in red)

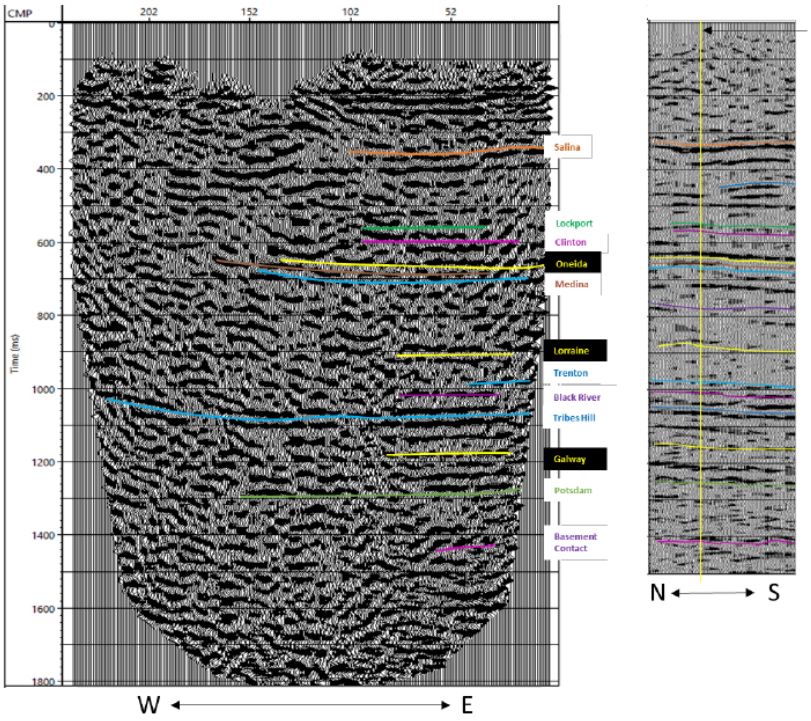

Figure 23: Left: Line 1/3/5/6 (Stevenson/Road Facilities) seismic time section after migration and FX deconvolution. Right: Interpretations of matching strong reflectors on the industry profile at a projected point of intersection. The pair of strong reflectors, between 1060 and 1100 ms, are interpreted to represent the same two strong reflectors straddling the blue line on the industry profile marking the Tribes Hill formation.

Line 2 (Game Farm Road)

The seismic sections thus far described are characterized by relatively continuous reflections that are readily correlated with geological units identified on industry seismic profiles. Reflection sections generated from some of the other shot and receiver lines tend to be less informative, with less distinct reflections or noisier images. Line 2 along the Game Farm Road (**Figure 24**) was problematic in this respect, possibly a result of large gaps in shot and receiver coverage (Figures 1, 3) and increased noise due to a higher volume of traffic on this road. The shot and receiver gaps were necessary to avoid disturbing a particularly sensitive facility, the Cornell Raptor center.

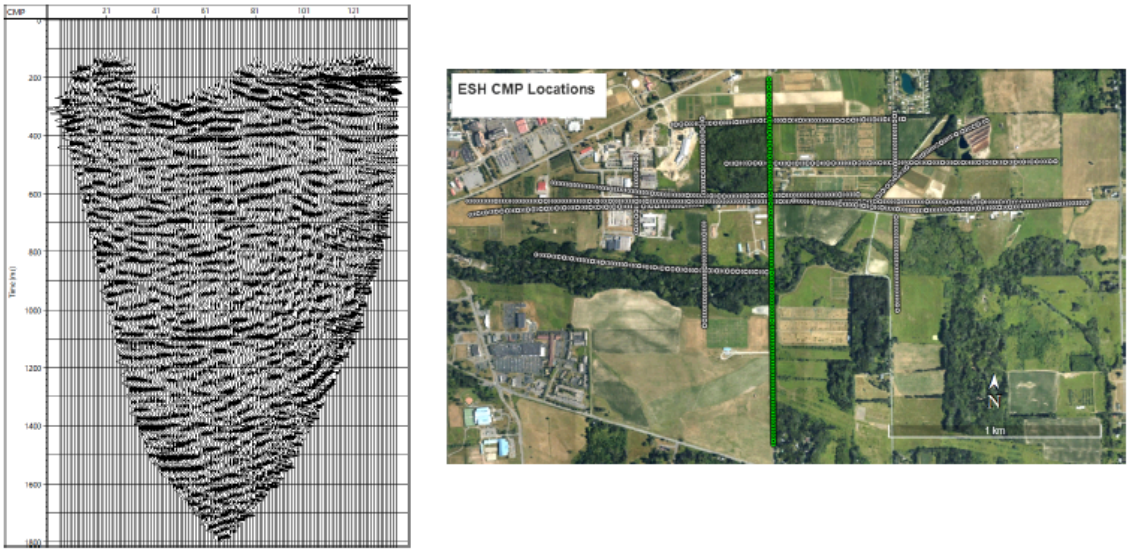

Figure 24: Left: Line 2 (Game Farm Road) seismic time section after migration and FX deconvolution. Orientation is west (left) to east (right) . Vertical axis is two-way travel time in milliseconds. Horizontal axis is labelled with the CMP bin number. CMP bins are spaced 12.5m apart. Right: Location of CMP (shown in red).

There are a few distinct reflection segments in the shallow subsurface, but the reflectors that correlate most convincingly with those on previous sections are the ones around 1060 and 1100 ms, which are again interpreted as the boundary between the Black River and the Tribes Hill Formations (**Figure 25**). Deeper reflection segments could plausibly be associated with the top of the Potsdam and the top of the Precambrian basement, but their short extent limits the utility of this identification.

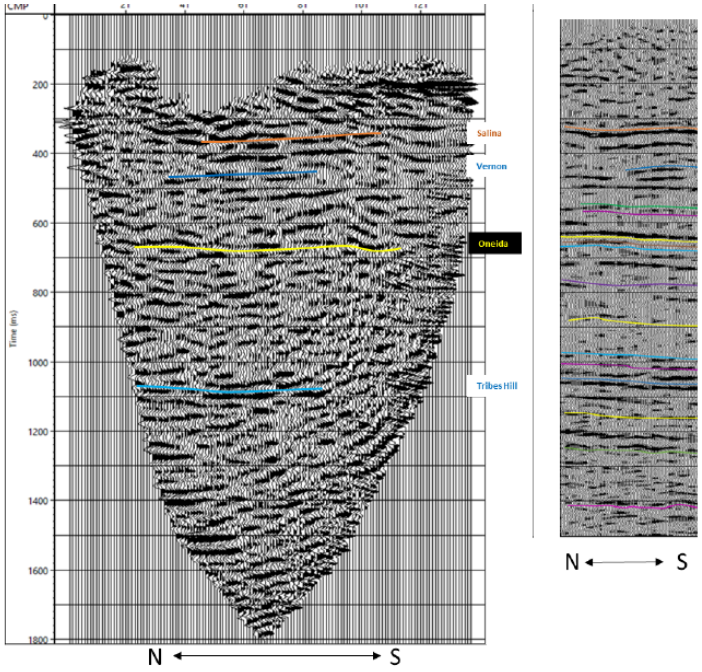

Figure 25: Left: Line 2 (Game Farm Road) seismic time section after migration and FX deconvolution and correlations with industry date on the right. (left). Right: Industry seismic line near but not intersection line 2. The interpretations corelates a discontinuous reflection at 1100 ms with the top of the Tribes Hill formation.

Line 3 (Recreation Trail)

Line 3 along the Recreation Trail also lacks the continuity of the better seismic lines, with particularly poor definition at shallow depths (**Figure 26**). The vibrator was operating at 50% power for this line, and the data collection was prematurely terminated when damage to the trail surface became evident.

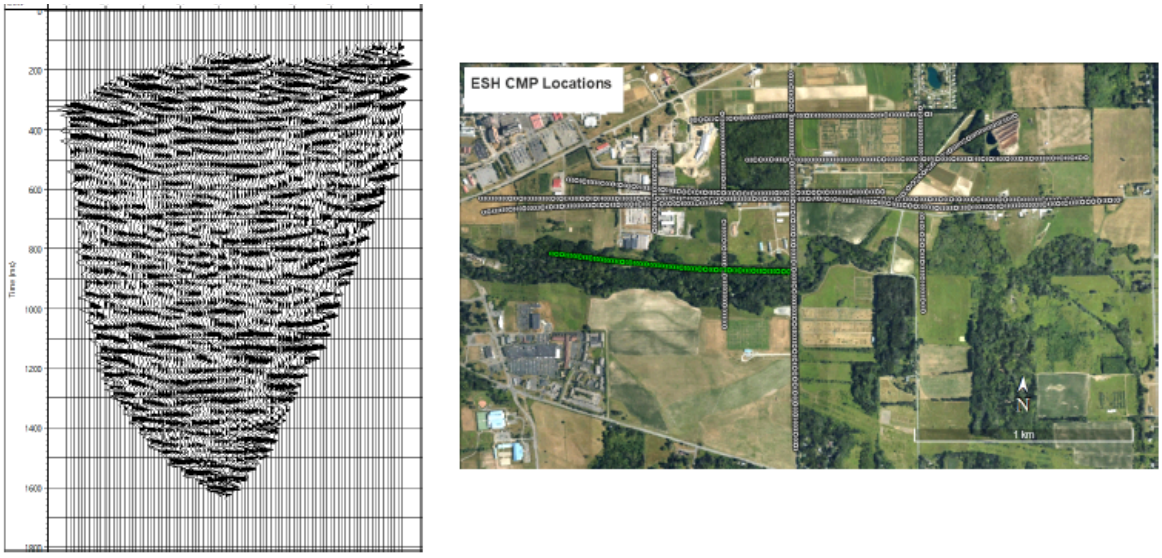

Figure 26: Left: Line 3 (Recreation Trail) seismic time section after migration and FX deconvolution. Oriented west (left) to east (right). Vertical axis is two-way travel time in milliseconds. Horizontal axis is labelled with the CMP bin numbers. CMP bins are spaced 12.5m apart. Right: Location of CMP line (marked in red).

Since none of the industry or Cornell profiles intersect the Recreation Trail line, identification of possible Tribes Hill and Potsdam reflections is based on their expected depths. A discontinuous band of reflections at about 1100 ms is likely to correspond to the top of the Tribes Hill Formation, and a slightly more continuous reflection at 1290 ms could correspond to the top of the Potsdam Formation **(Figure 27)**. Again, very little can be confidently interpreted in the shallow section and a reflection marking the top of basement is not obvious.

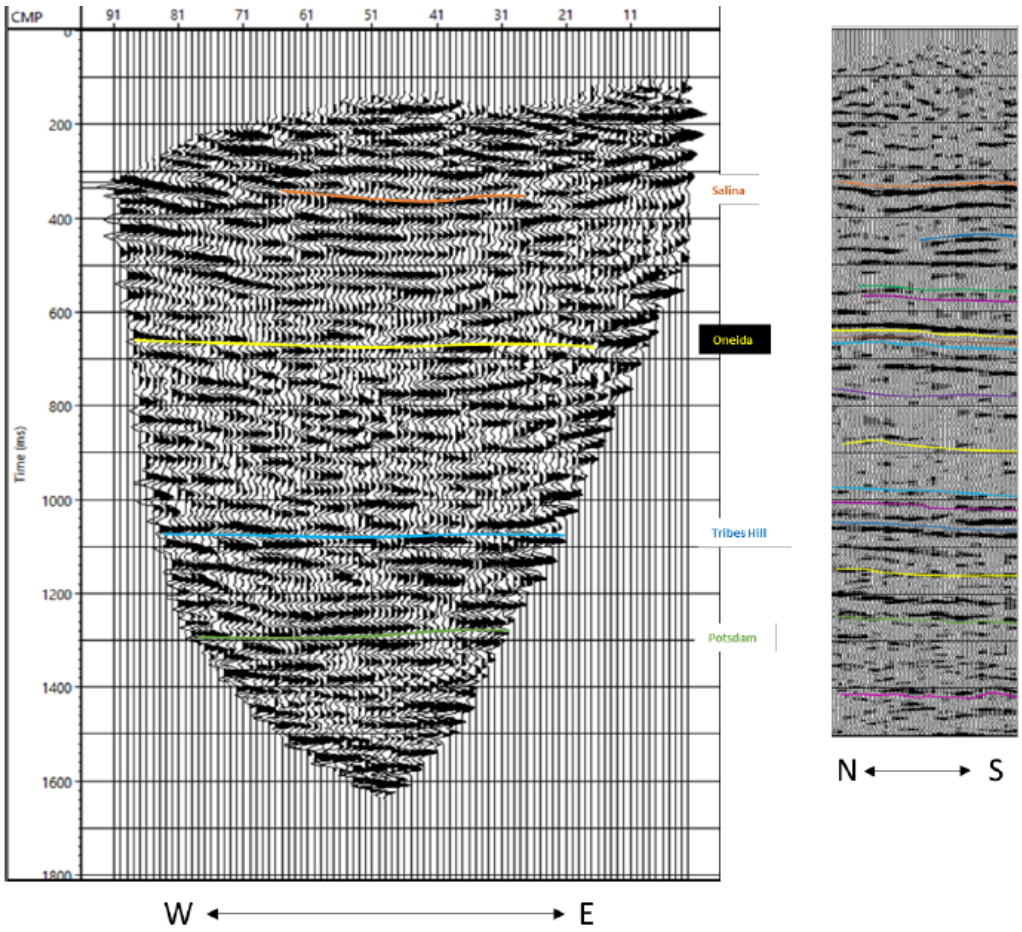

Figure 27: Left: Line 3 (Recreation Trail) seismic time section after migration and FX deconvolution (left). Right Industry seismic line near but not intersection line 2. The relative lack of coherent reflections make interpretation difficult, though some deeper events may correspond to the top of the Tribes Hill and Potsdam Formation based on correlations to the industry section.

Line 4 (Compost Facility Road)

Due to the presence of buildings associated with Cornell's Compost Facility, as well as the termination of the road approximately halfway along the line of receivers, sources were restricted to a relatively small portion of Line 4. The resulting low stacking fold may be responsible for the relative lack of interpretable reflections (**Figure 28**). In addition, the bend approximately halfway through the line (**Figure 28**) resulted in a lateral scatter of the common mid-points which may also have contributed to the poor quality of the stacked section. In order to maximize the stacking fold, the length of the bins was extended laterally, capturing more of

the scattered midpoints within each bin, but also increasing the likelihood that heterogeneity within the bins has degraded the stack signal.

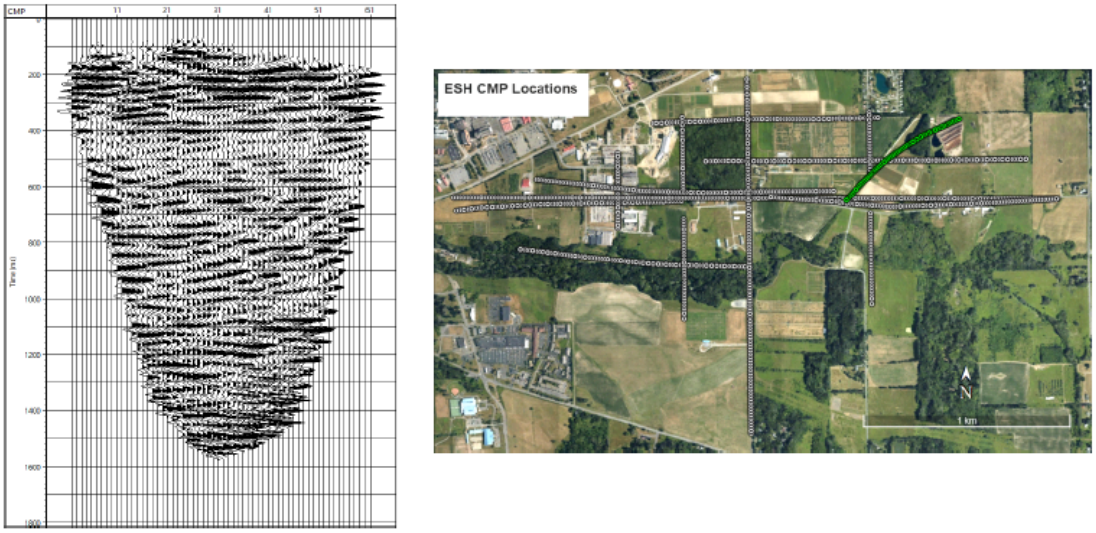

Figure 28: Left: Line 4 (Compost Facility Road) seismic time section after migration and FX deconvolution. Orientation is southwest (left) to northeast (right). Vertical axis is two-way travel time in milliseconds. The horizontal axis is labelled with the CMP bin numbers. CMP bins are spaced 12.5m apart. Right: Location of the CMP line (marked in red) .

Few shallow reflections can be distinctly traced across the section. There is a somewhat continuous reflection dipping southwest from 1080 to 1100 ms. We interpret this reflection (**Figure 29**) to correspond to the deeper of the reflections in the pair that marks the top of the Tribes Hill Formation on industry and the other ESH lines, especially Line 2 (Stevenson Road).

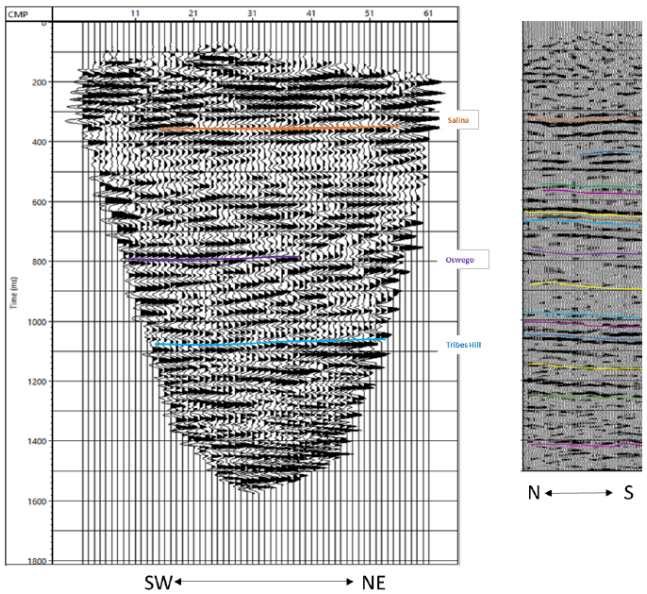

Figure 29: Left: Line 4 (Compost Facility Road) seismic time section after migration and FX deconvolution. Reflectivity is relatively discontinuous. Right: Industry seismic line near but not intersecting line 4. The reflection at 1080 ms corresponds to the deeper of the two strong reflectors that mark top of the Tribes Hill on the industry seismic section.

Line 2/7 (Game Farm Parallel West)

Shots from Game Farm Road and receivers along Solidago Road were used to image the subsurface between these two lines. As a result of the gap in the shots along Game Farm Road, a similar gap appears in the common midpoint location. This gap is marked with a vertical yellow line in the time section in **Figure 30** and shown on the accompanying map.

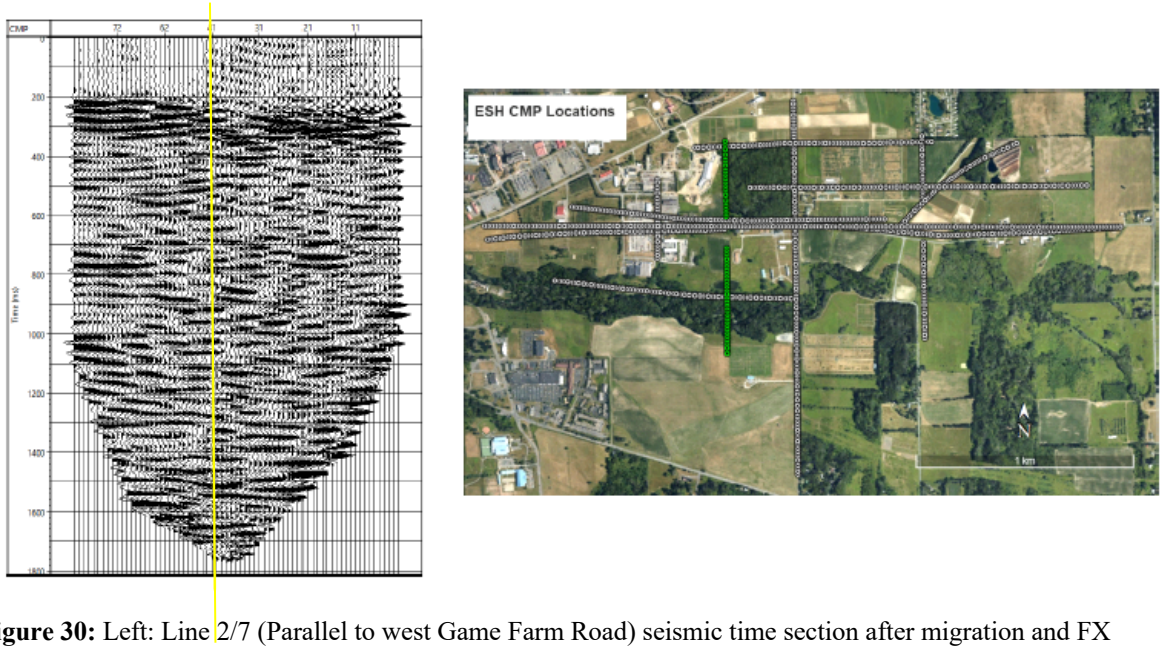

Figure 30: Left: Line 2/7 (Parallel to west Game Farm Road) seismic time section after migration and FX deconvolution. Oriented north (left) to south (right). Vertical axis is two-way travel time in milliseconds. The horizontal axis is labelled with the CMP bin numbers. CMP bins are spaced 12.5m apart. The yellow line marks a gap in imagery due to gaps in the shot point coverage. Right: Location of CMP line (marked in red).

The lack of reflector definition and continuity renders any interpretation of this line speculative at best. The correlations shown in **Figure 31** are reasonable extrapolations. Nevertheless, there is a low degree of confidence in the association of specific reflectors on the seismic section to geological unit as the much of the apparent continuity may be an artifact of migration and FX deconvolution filters.

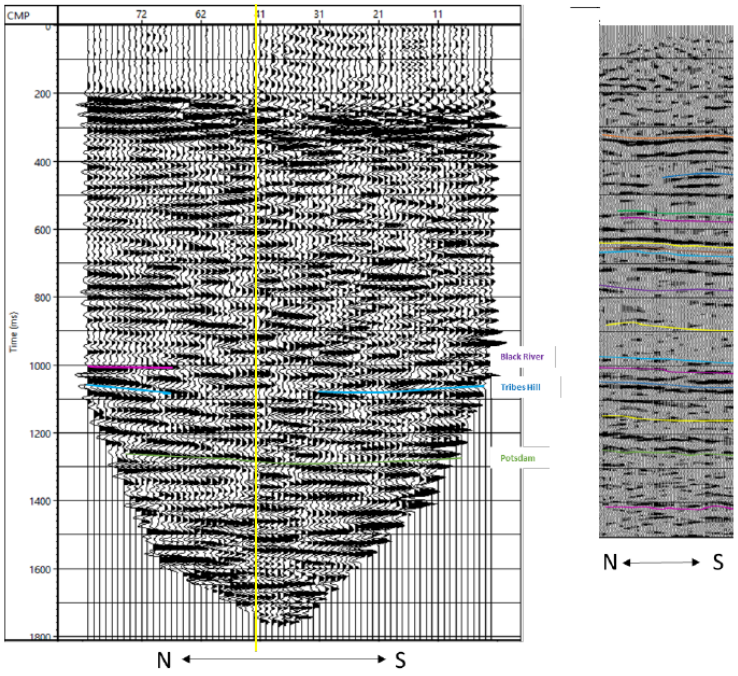

Figure 31: Left: Line 2/7 (West parallel to Game Farm Road) seismic time section after migration and FX deconvolution. Right: Industry seismic line with interpretation. The lack of reflector continuity renders the correlations shown here with industry data speculative.

Line 2/9 (Game Farm Parallel East)

The shots along Game Farm Road and recorded by receivers along Line 9 were used to produce a short seismic profile perpendicular to Stevenson Road (**Figure 32**). A vertical yellow line on the time section marks the gap between the two segments which make up this line.

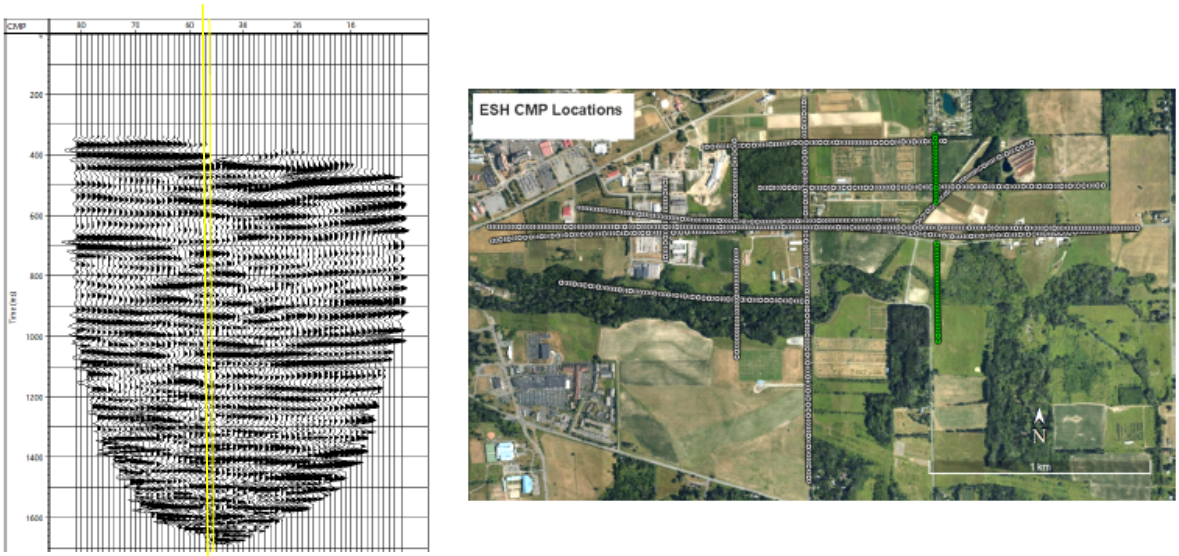

Figure 32: Left: Line 2/9 (East Parallel to Game Farm Road) seismic time section after migration and FX deconvolution. Oriented north (left) to south (right) . Vertical axis is two-way travel time in milliseconds. The horizontal axis is labelled with the CMP bin locations. CMP bins are spaced 12.5m apart. Right: Location of CMP line (marked in red) . Note the large gap in the center of the line.

Though the geometry and processing flow used for this line are nearly identical to those used for the previous line, this profile appears to show more coherent, albeit short, reflections and less noise. It is possible that this line benefited from slightly greater offsets than the previous Line 2/7, or from reduced noise a result of the receivers being in an isolated field as opposed to along a road used heavily by traffic. However, the large offset and low stacking fold have resulted in the stacked section being more sensitive to the stacking velocity model used. The reflections we associate with the boundary between the Black River and Tribes Hill based on seismic character (**Figure 33**) are approximately 18 ms deeper on this profile than on its intersection with the west end of Line 5 (McGowan Road).

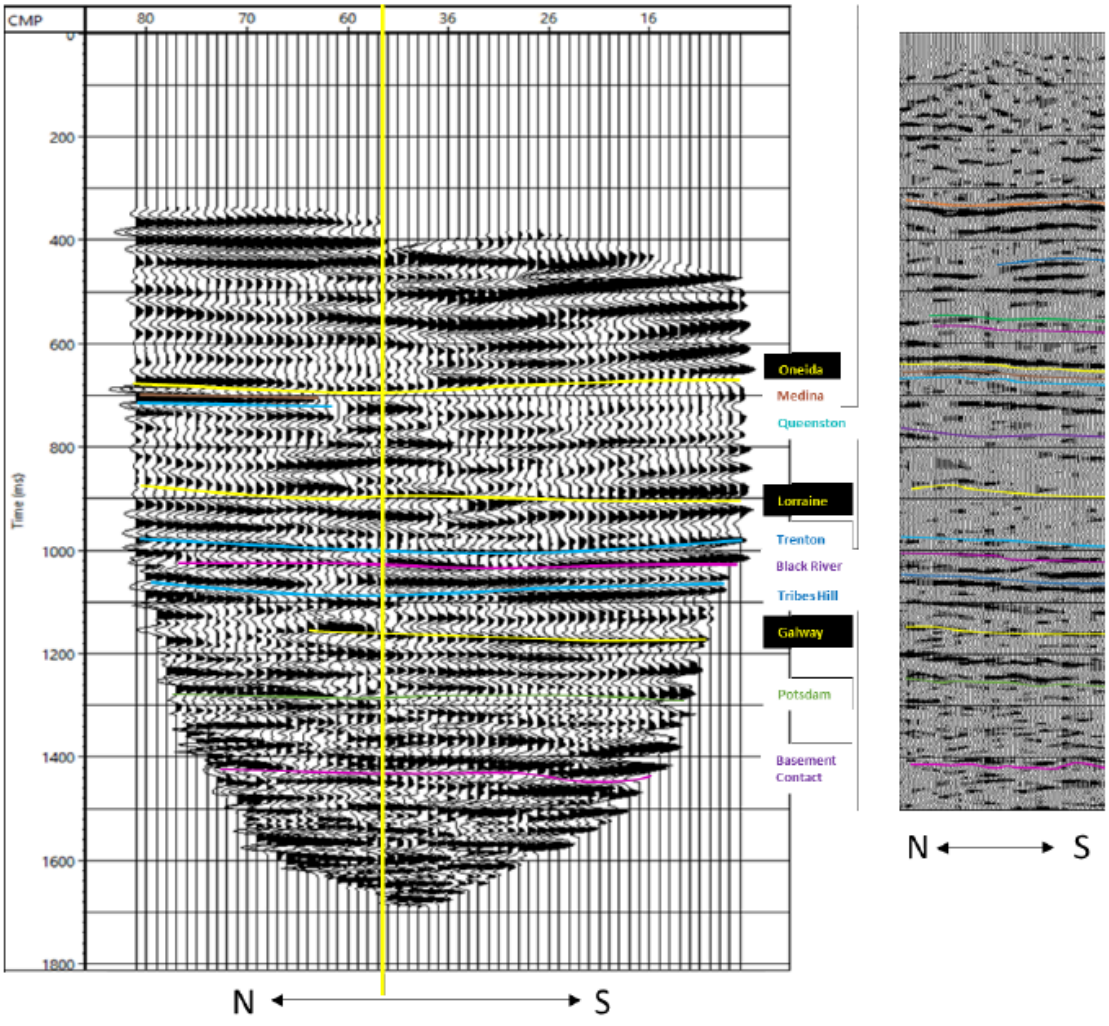

Figure 33: Left: Line 2/9 (East Parallel to Game Farm Road) seismic time section after migration and FX deconvolution. Right: Industry seismic profile. Reflectors at 1040 and 1080 ms on line 29 are interpreted to correspond to the reflection pair on industry seismic sections straddle the contact between the Black River and Tribes Hill formations.

Intercomparison of ESH Seismic Time Sections

Figure 34a displays the time sections for three parallel lines- 5 (McGowan Woods Road), 1/5 (Stevenson Parallel), and 1 (Stevenson Road)- to emphasize the correlation of reflection between them. These three lines, all oriented from west to east, are approximately

perpendicular to an industry line that passes near the east end of Stevenson Road (**Figure 34b**) . These lines are spaced approximately 200 m apart. The last (rightmost) traces in these profiles show clear deep reflections that are approximately 790, 270, and 370 m in horizontal distance from the projected intersection of these lines with the industry line, respectively.

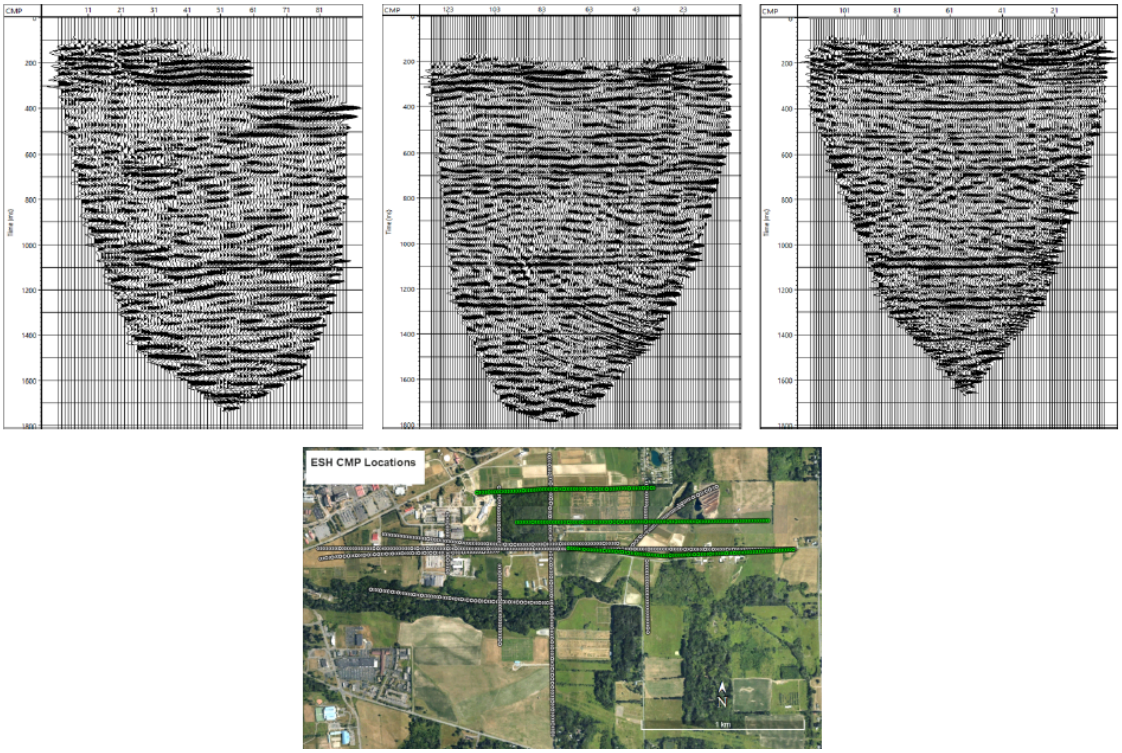

Figure 34: A: (From left to right) Line 5 (McGowan Woods Rd), Line 1/5 (Stevenson Parallel, and Line 1 (Stevenson Road) seismic time sections. Each section is oriented from west to east. Comparison of these three Cornell seismic lines shows of southward dip when looking at the more coherent, deeper reflectors. This is consistent with what is seen in the nearby industry profiles. B: CMP positions for Lines 5, 1/5 and 1.

Careful correlation of the key reflections between these lines confirms the expected southward dip of the Paleozoic strata. This is most obvious when looking at the reflections interpreted as the top of the Tribes Hill Formation, which appear deeper on Line 1 (Stevenson Road line, rightmost in **Figure 5**) than the Line 5(McGowan Woods line, leftmost in **Figure 5**). Another key observation is a subtle westward dip seen in all three profiles, once again most evident for the Tribes Hill reflections.

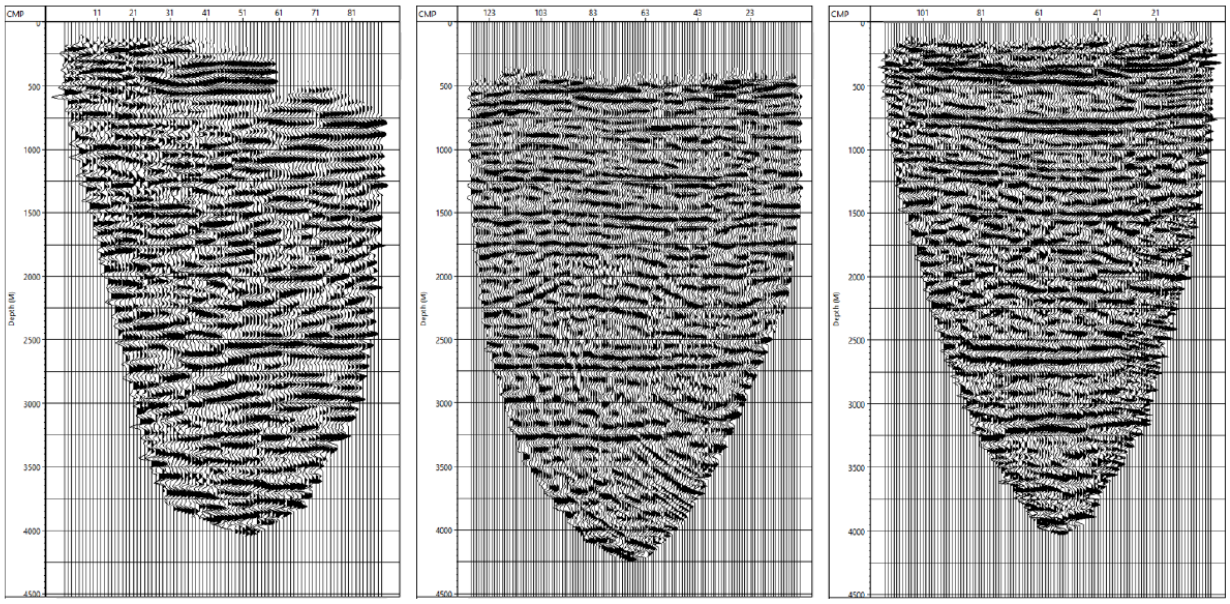

Figure 35: From Left to Right: Depth sections for Line 5 (McGowan Woods Road), Line 1/5 (Stevenson Parallel), and Line 1 Stevenson Road. The vertical axis is in meters relative to a fixed datum of 290 m. The horizontal axis is labelled with CMP bin numbers. CMP bins are spaced 12.5 m apart. In each profile, west is to the left and east is to the right.

Intercomparison of ESH Seismic Depth Sections

Depth converted versions of the seismic time sections in **Figure 34** are shown in **Figure 35.** The depth position of reflections is highly sensitive to the velocity model used for conversion. Smoothed versions of the stacking velocity picks for each of the lines were used to create these depth sections.

Carrying over the interpretations made on the time sections, the reflector just below the contact between the Black River and Tribes Hill would be placed around 2550, 2725, and 2650 m below the 290 m reference datum for McGowan Woods Road, Stevenson Parallel, and Stevenson Road, respectively.

Contour Map of Top of Tribes Hill Formation

In a first attempt to represent the three-dimensional variation in stratigraphy revealed by comparison of the ESH vibroseis and industry seismic profiles, a contour map of the travel time to the top of the Tribes Hill Formation, one of the most easily identified reflectors, was generated (**Figure 36)**. These contours confirm the expected general southward dip in the Paleozoic strata. However, they also suggest a significant southwestward dip in the eastern part of the study area.

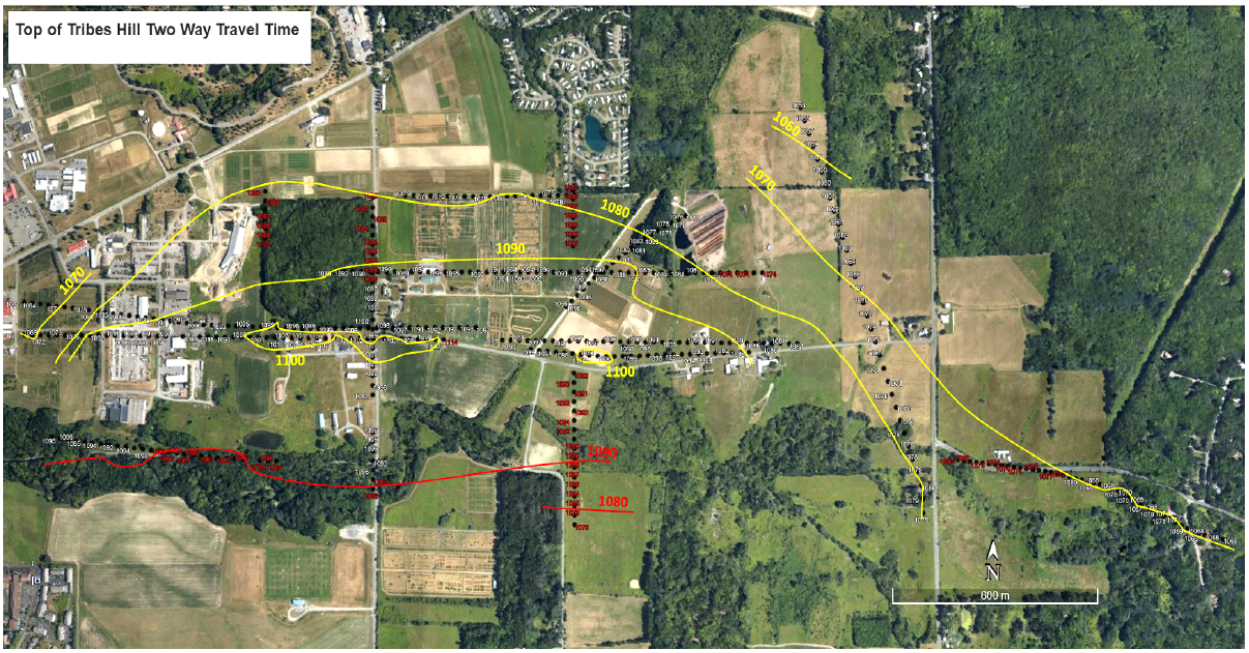

Figure 36: Contours of the two-way travel time for the reflection from the top of the Tribes Hill Formation. Contour interval is 10 ms. Red contours indicate areas where the reflector is poorly defined by the seismic data. Dots corresponds to CMP coverage of the various profiles. The two easternmost lines are industry profiles shifted to the same datum as the Cornell lines.

Structure Within the Paleozoic Strata.

For the most part, the Paleozoic strata revealed by the Cornell vibroseis reflection profiles, where well imaged and below the relatively shallow salt formations, is subhorizontally layered and undisrupted by any large-scale faulting. This stratigraphy is most confidently imaged east of Game Farm Road and at depths between 500 and 3500m. Correlating these data with regional oil and gas seismic sections suggests a broad fold, evidenced by southwestward dipping reflections (**Figure 36**) near the eastern margin of the survey area. However, reflector continuity is highly variable due to variations in data quality, and the presence of small-scale(e.g. 500m or less) offsets cannot be ruled out for all of the seismic lines.

The Precambrian Basement

The nature of the crystalline basement in the vicinity of the candidate ESH drilling sites is also of particular interest. Although some of the Cornell vibroseis lines discussed in this report feature reflectors that may correspond to the top of the Precambrian basement, the aperture of the surveys imposed by the limited physical access caused interference by surface wave noise resulted in little useful imagery of the sub-sedimentary.

Conclusions

A series of relatively short multichannel seismic reflection profiles were collected in the immediate vicinity of candidate locations for drilling related to the Cornell Earth Source Heating project. Data quality is variable among the seismic reflection images produced from these profiles due to the limited aperture allowed by logistical access and resulting surface wave noise.

However, the basic stratigraphy near candidate sites is well defined and correlatable to regional seismic results previously collected for oil and gas surveys. Overall, the seismic imagery confirms the expectation of a relatively simple southward dip[ping sedimentary sequence, though with a broad fold resulting in southwestward dips at the eastern border of the survey area. Major fault offsets of the well imaged strata are absent, although reflector continuity on some of the seismic images is too poor to preclude faults with small vertical offsets (e.g. <500m) .

Acknowledgements

This work was supported by the College of Engineering at Cornell University. The assistance and involvement of faculty and staff at the NEES vibroseis facility at the University of Texas at Austin, contributed much to the success of this work. The efforts of numerous Cornell undergraduates during the deployment of the seismic stations used to collect the data analyzed in this report is gratefully acknowledged. The assistance of technical staff from SAExploration in training these students in the deployment and operation of the Zland nodes is also much appreciated.

References

May, D., and L. Brown 2019, Investigation of background vibrations in Cornell University's mouse facilities using ZLand GenII nodes. Technical Report.

Reynolds, J.M. , 2011, An Introduction to Applied and Environmental Geophysics, (2nd Ed) , Wiley and Sons, New York

Waters, K., H. 1992, Reflection seismology: A Tool for Energy Resource Exploration, (3rd Ed) Krieger Publishing Co., Malabar.

Yilmaz, O., 1987, Seismic Data Processing, Soc. Exploration Geophysicists, Tulsa.

Appendix I: Seismic Profiles

Line 1 (Stevenson Road)

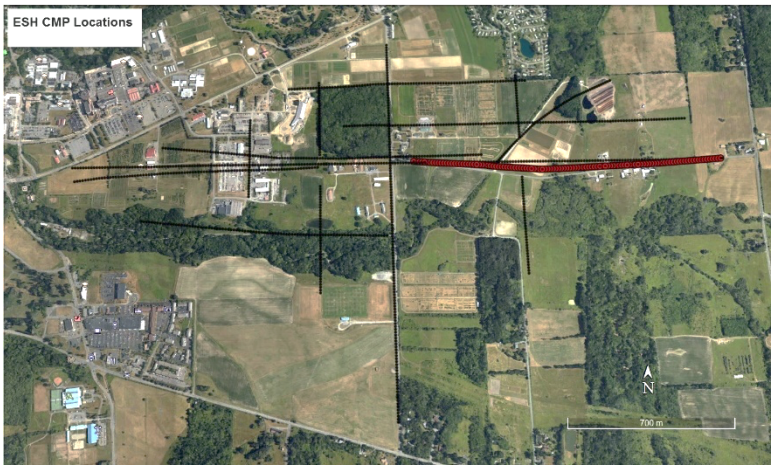

Figure 37: Map showing common midpoint locations for the Stevenson Road line marked in red.

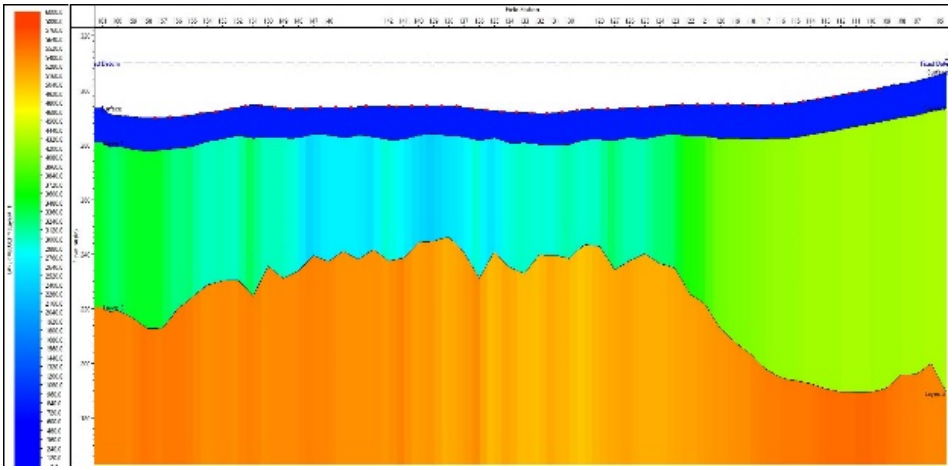

Figure 38: Refraction model created for Stevenson Road oriented West-East. A weathering layer of 800 m/s was assumed and is represented by a thin blue layer.

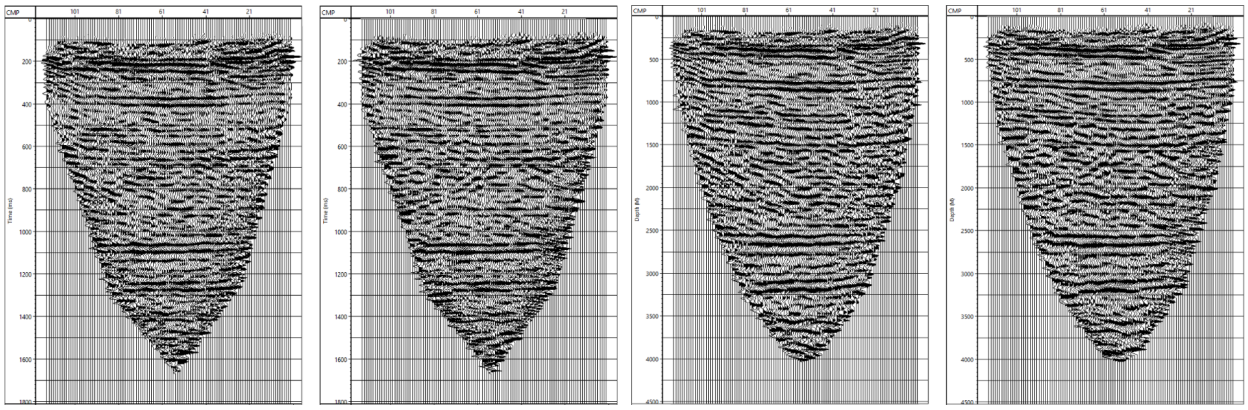

Figure 39: From left to right, unmigrated and migrated time sections after FX Deconvolution and the corresponing depth sections without and without migration.

Line 2 (Game Farm Road)

Figure 40: Map showing common midpoint locations for the Game Farm Road line marked in red.

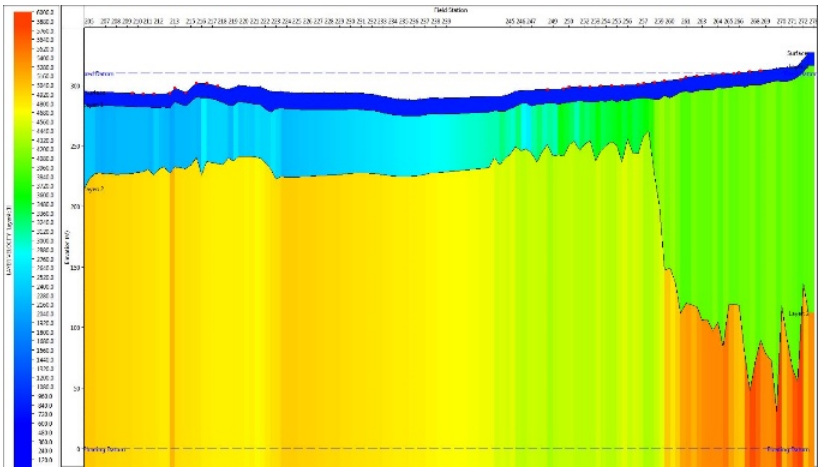

Figure 41: Refraction model created for Game Farm Road oriented North-South. A weathering layer of 800 m/s was assumed and is represented by a thin blue layer.

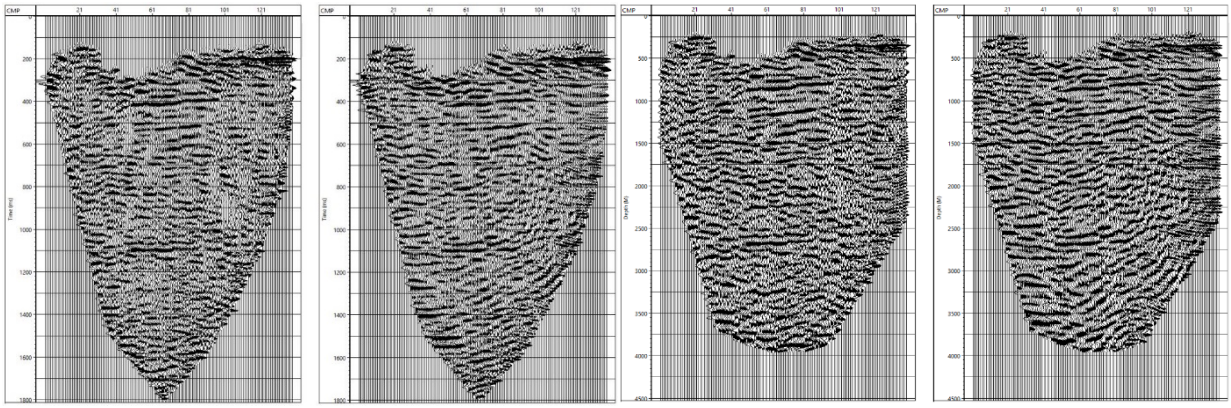

Figure 42: From left to right, unmigrated and migrated time sections after FX Deconvolution and the corresponing depth sections without and without migration.

Line 3 (Recreation Trail)

Figure 43: Map showing common midpoint locations for the Recreation Trail line marked in red.

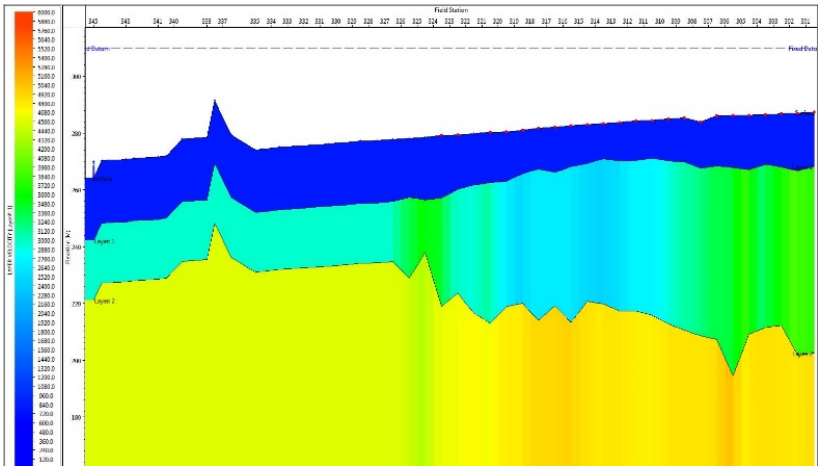

Figure 44: Refraction model created for the Recreation Trail oriented West-East. A weathering layer of 800 m/s was assumed and is represented by a thin blue layer.

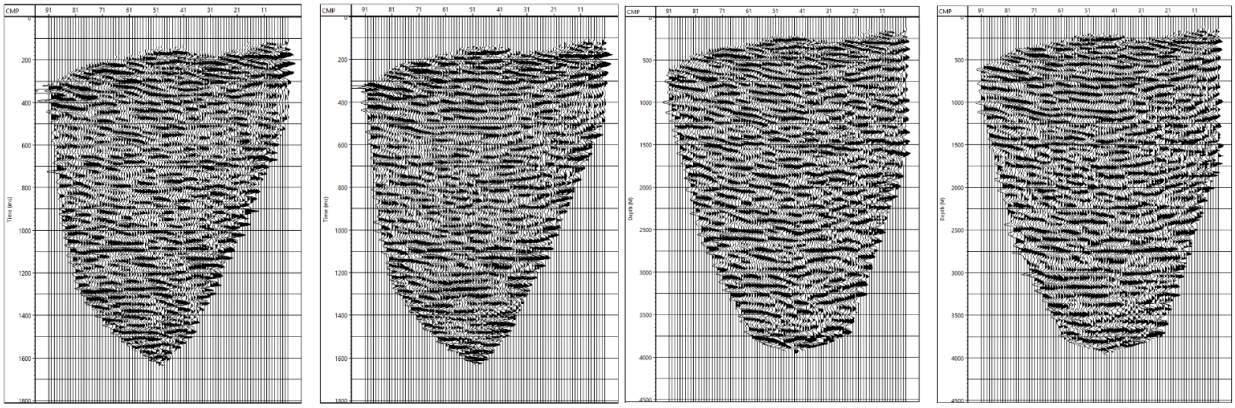

Figure 45: From left to right, unmigrated and migrated time sections after FX Deconvolution and the corresponing depth sections without and without migration.

Line 4 (Compost Facility Road)

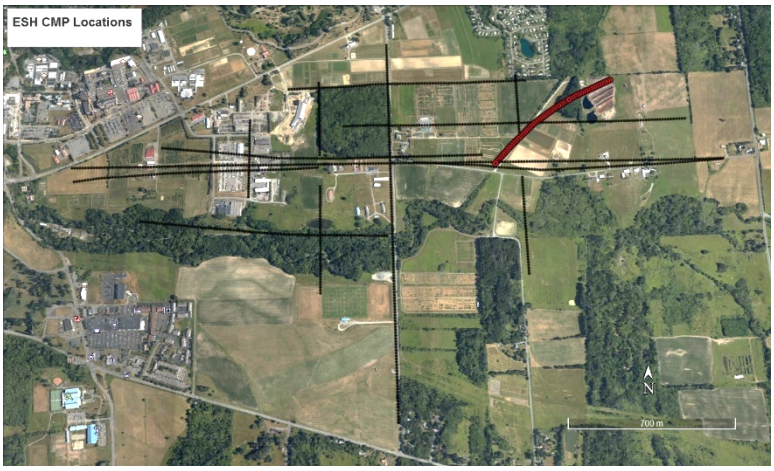

Figure 46: Map showing common midpoint locations for the Compost Facility line marked in red.

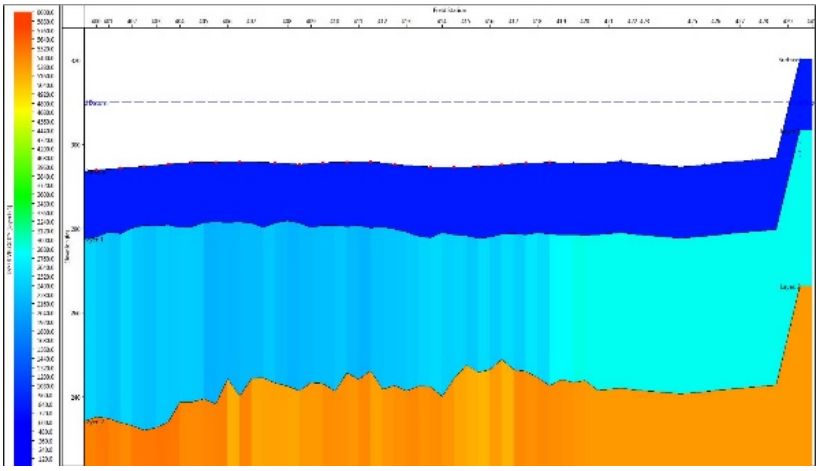

Figure 47: Refraction model created for the Compost Facility oriented Southwest-Northeast. A weathering layer of 800 m/s was assumed and is represented by a thin blue layer.

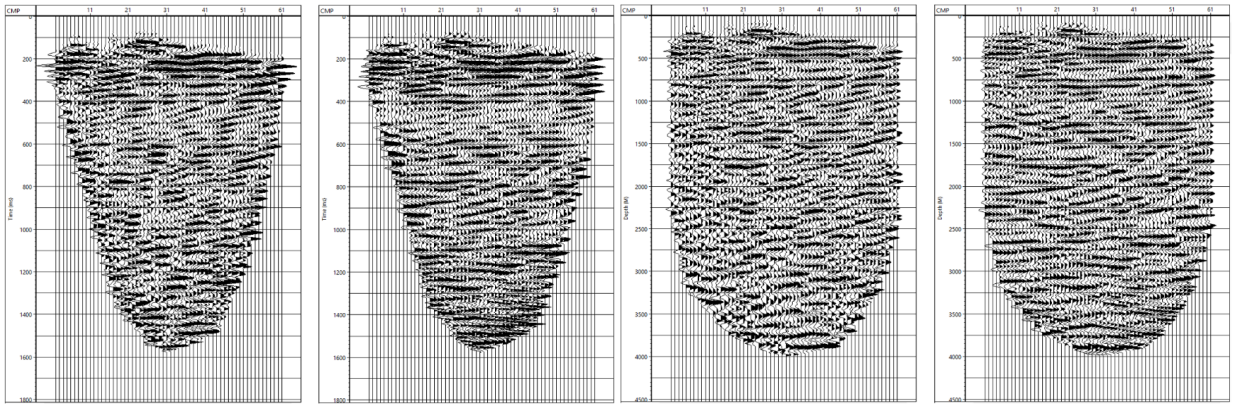

Figure 48: From left to right, unmigrated and migrated time sections after FX Deconvolution and the corresponing depth sections without and without migration.

Line 5 (McGowan Woods Road)

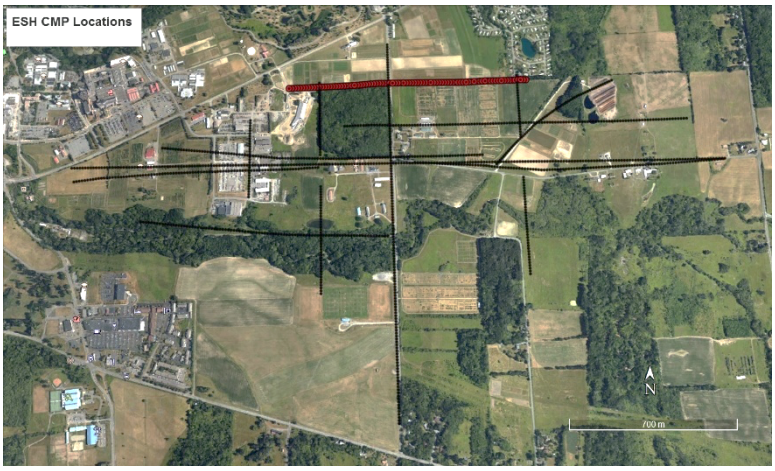

Figure 49: Map showing common midpoint locations for McGowan Woods Road line marked in red.

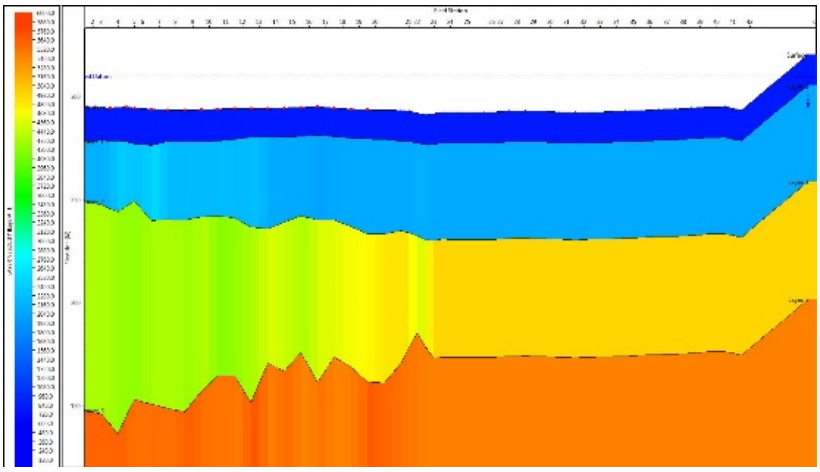

Figure 50: Refraction model created for McGowan Woods Road oriented West-East. A weathering layer of 800 m/s was assumed and is represented by a thin blue layer.

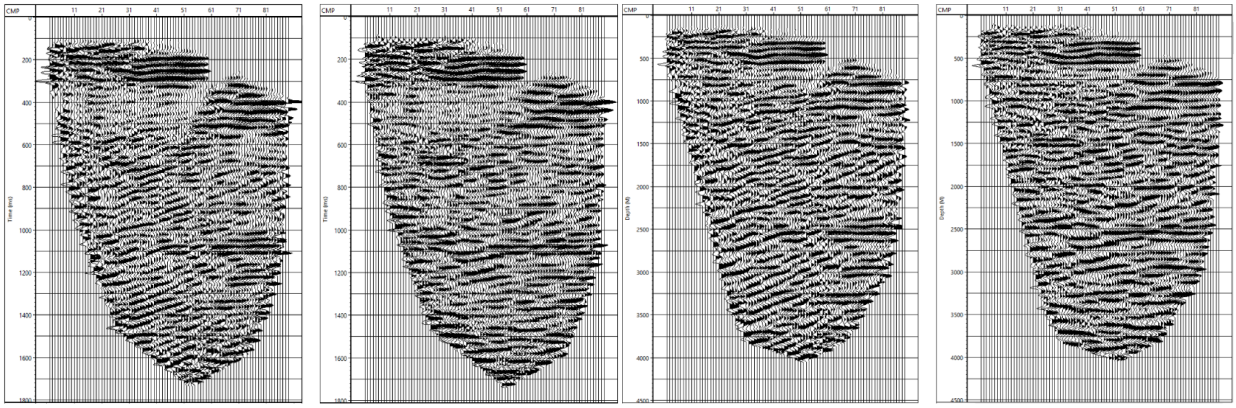

Figure 51: From left to right, unmigrated and migrated time sections after FX Deconvolution and the corresponing depth sections without and without migration.

Line 6 (Cornell Orchards)

Figure 52: Map showing common midpoint locations for Cornell Orchards line marked in red. This line was excluded from earlier analysis and the countour map due to poor quality.

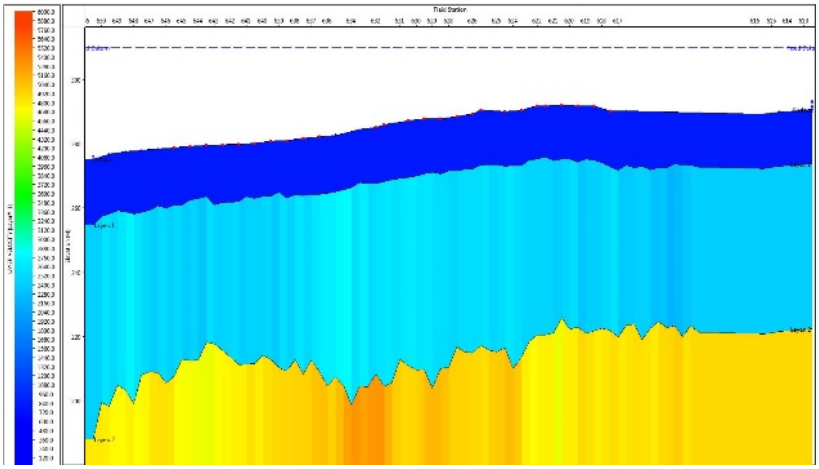

Figure 53: Refraction model created for the Cornell Orchards oriented West-East. A weathering layer of 800 m/s was assumed and is represented by a thin blue layer.

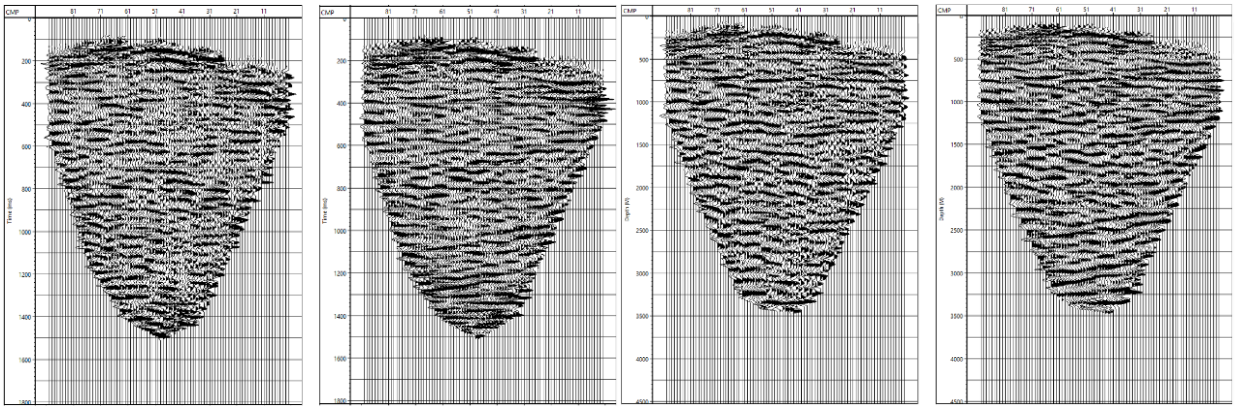

Figure 54: From left to right, unmigrated and migrated time sections after FX Deconvolution and the corresponing depth sections without and without migration.

Line 7 (Solidago Road)

Figure 55: Map showing common midpoint locations for Solidago Road line marked in red. This line was excluded from earlier analysis and the countour map due to poor quality.

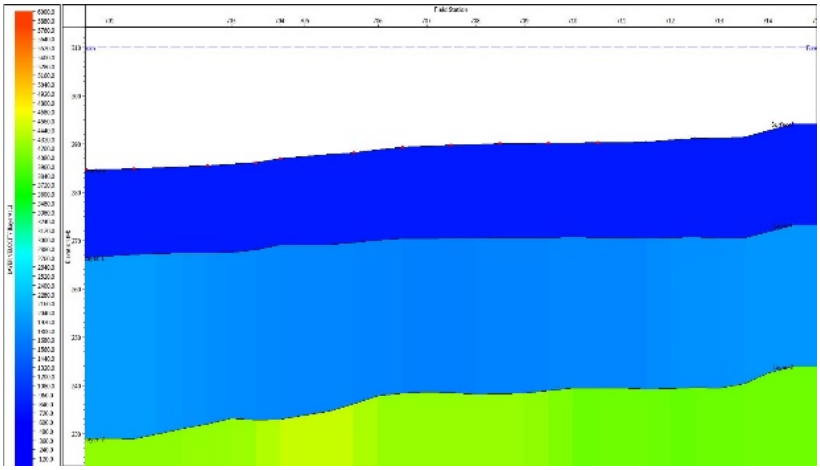

Figure 56: Refraction model created for Solidago Road oriented North-South. A weathering layer of 800 m/s was assumed and is represented by a thin blue layer.

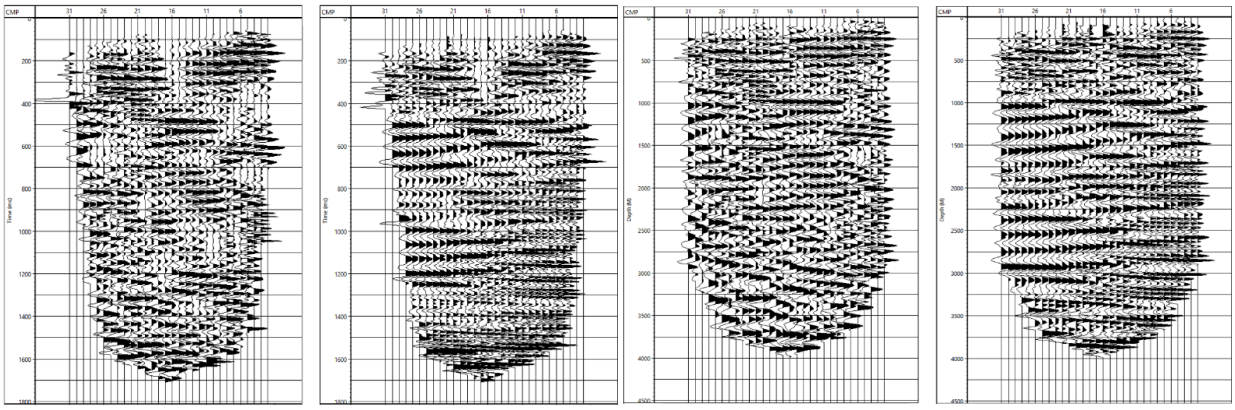

Figure 57: From left to right, unmigrated and migrated time sections after FX Deconvolution and the corresponing depth sections without and without migration.

Line 1/5 (Stevenson Parallel)

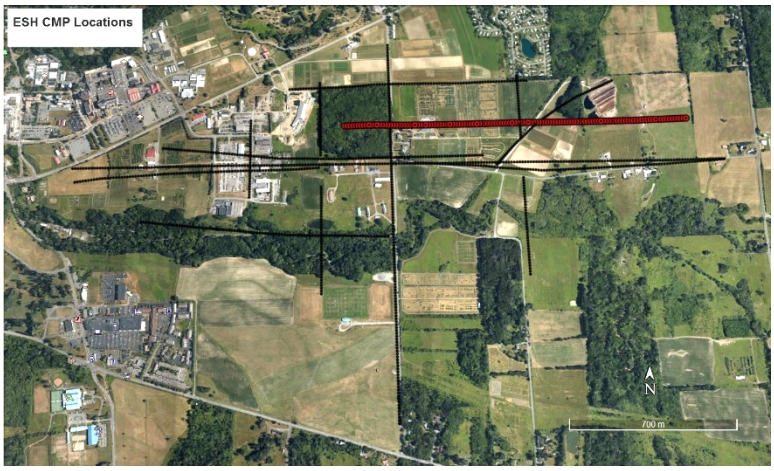

Figure 58: Map showing common midpoint locations for Stevenson Parallel marked in red.

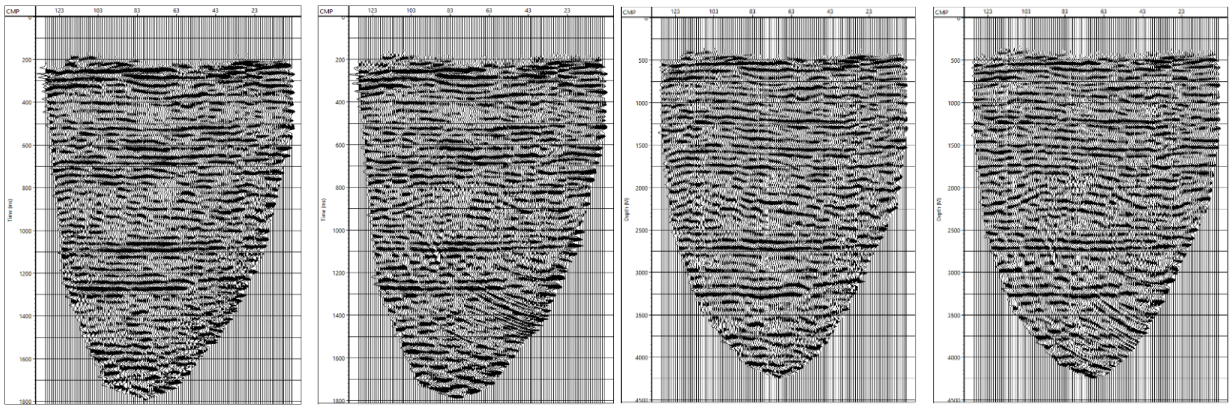

Figure 59: From left to right, unmigrated and migrated time sections after FX Deconvolution and the corresponing depth sections without and without migration.

Line 3/5 (Recreation Trail Parallel)

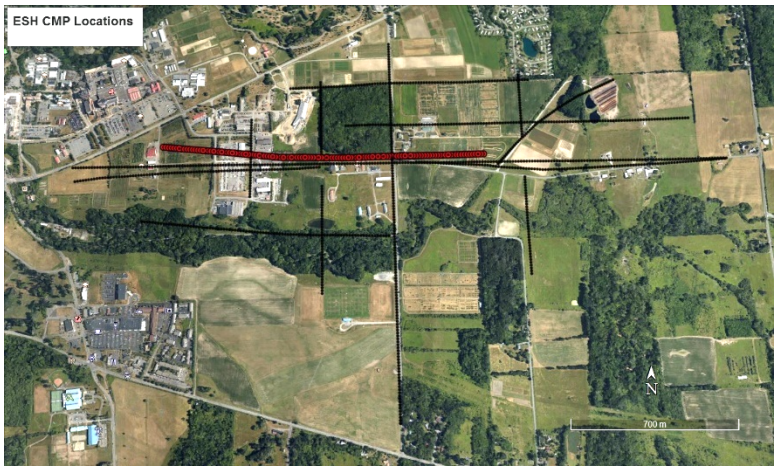

Figure 60: Map showing common midpoint locations for Recreation Trail Parallel marked in red.

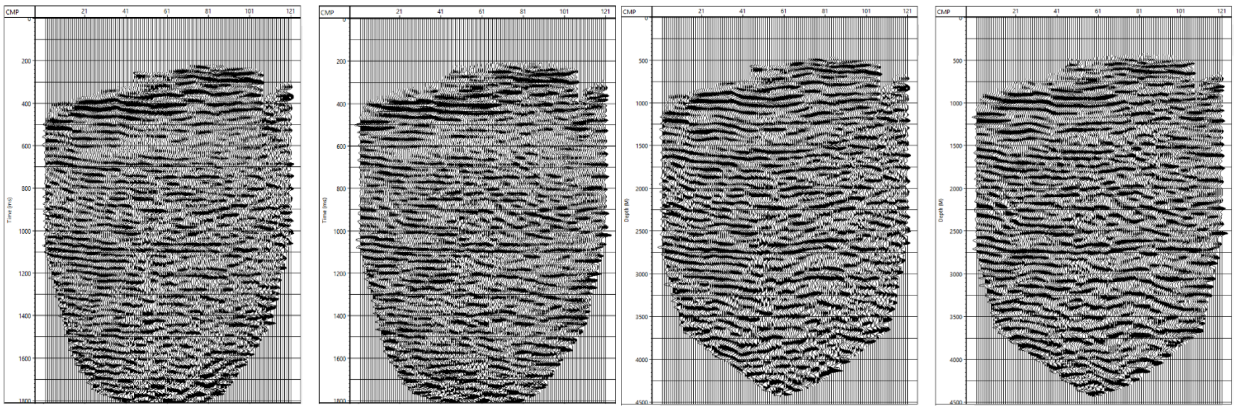

Figure 61: From left to right, unmigrated and migrated time sections after FX Deconvolution and the corresponing depth sections without and without migration.

Line 1/3/5/6 (Stevenson/Facilities)

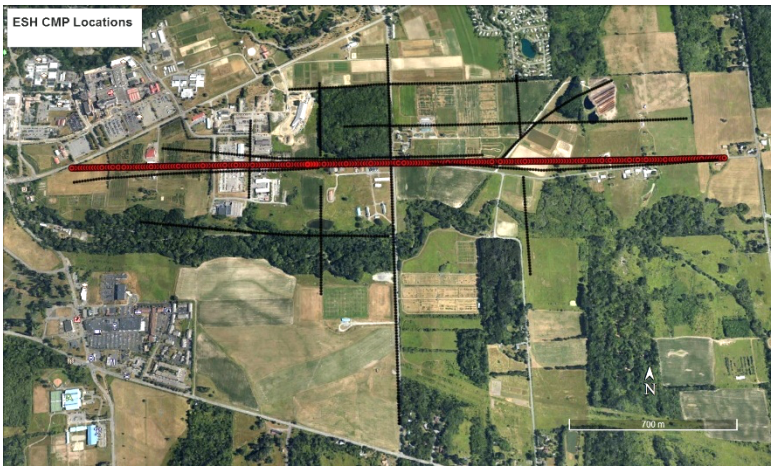

Figure 62: Map showing common midpoint locations for Facilities/Stevenson line marked in red.

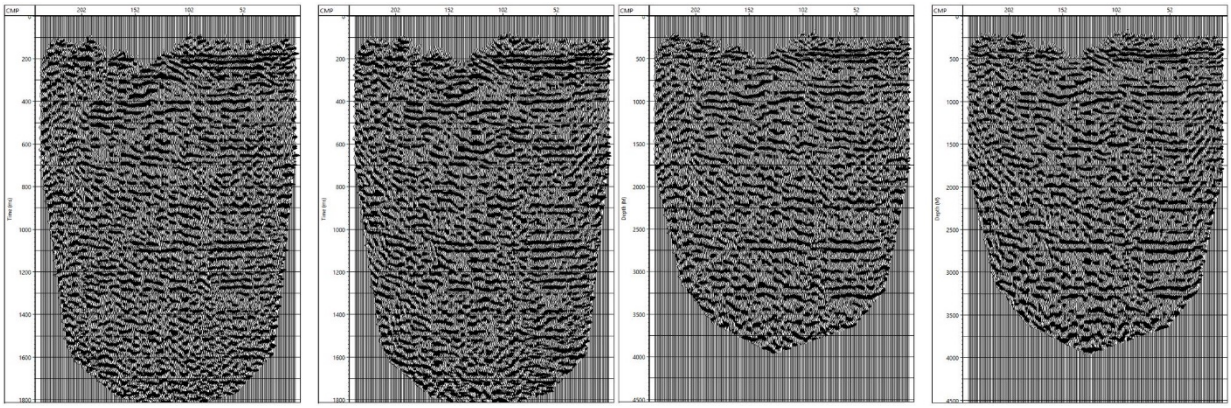

Figure 63: From left to right, unmigrated and migrated time sections after FX Deconvolution and the corresponing depth sections without and without migration.

Line 2/7 (Game Farm Road Parallel West)

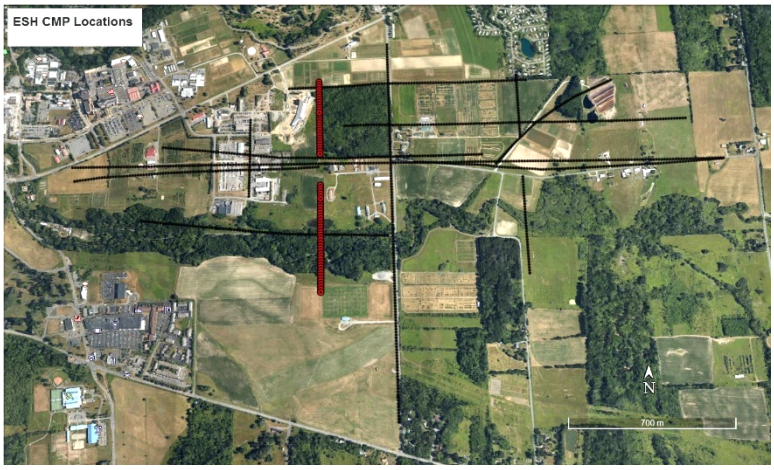

Figure 64: Map showing common midpoint locations for Game Farm Parallel West marked in red.

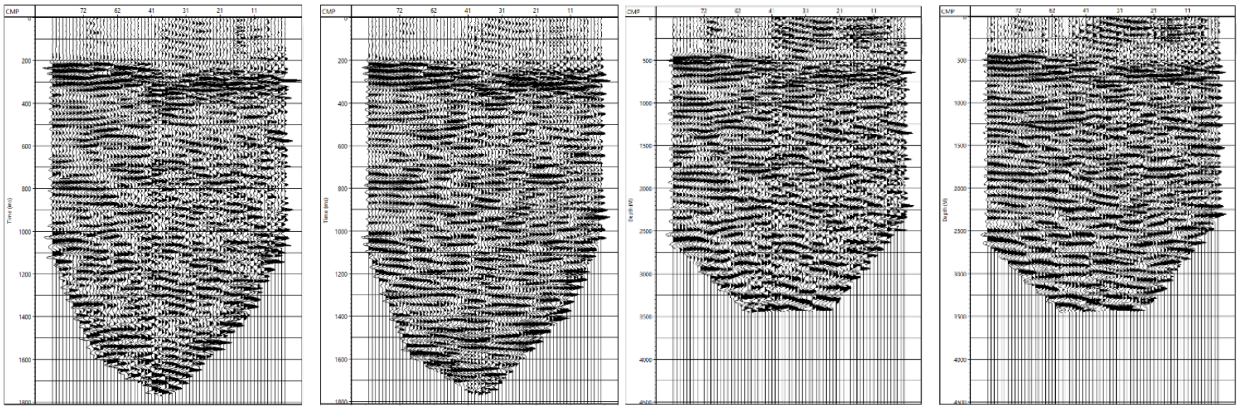

Figure 65: From left to right, unmigrated and migrated time sections after FX Deconvolution and the corresponing depth sections without and without migration.

Line 2/9 (Game Farm Road Parallel East)

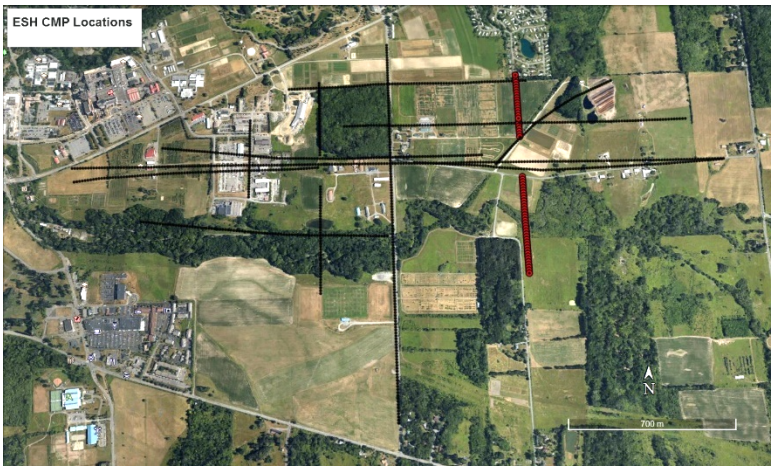

Figure 66: Map showing common midpoint locations for Game Farm Parallel East marked in red.

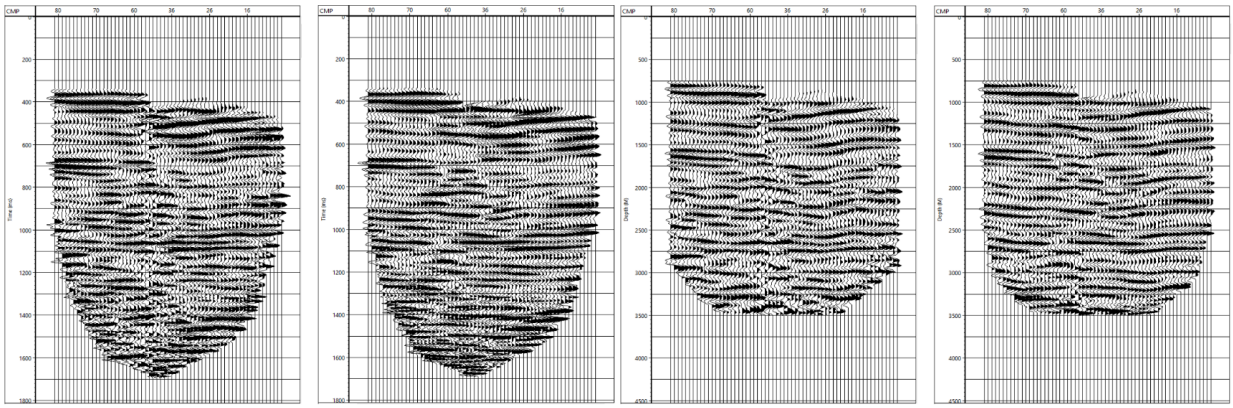

Figure 67: From left to right, unmigrated and migrated time sections after FX Deconvolution and the corresponing depth sections without and without migration.

Appendix II: Earthquake Records

Dryden High School Seismometer
Event Location: Decatur, TN, USA
Event Time: 09:14:43 UTC December 12th, 2018
Magnitude: 4.4

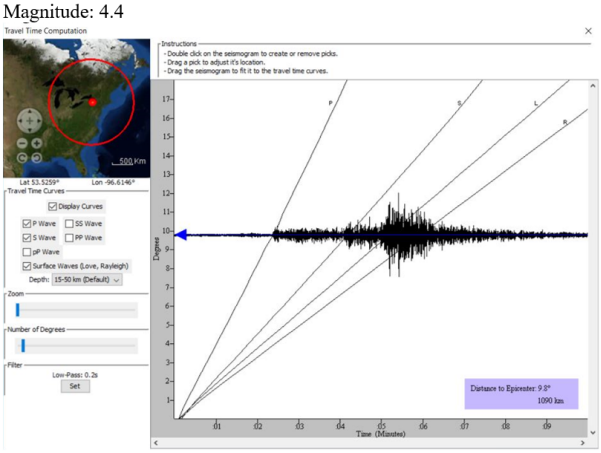

Dryden High School Seismometer
Event Location: Vancouver Island, BC, Canada
Event Time: 06:16:36 UTC October 22nd, 2018
Magnitude: 6.8

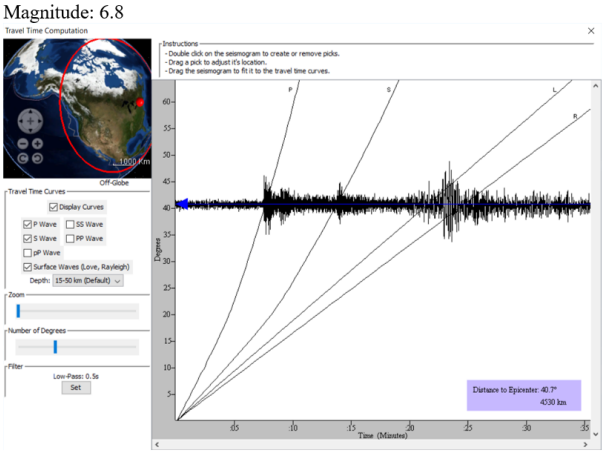

Ithaca High School Seismometer
Event Location: Vancouver Island, BC, Canada
Event Time: 06:16:36 UTC October 22nd, 2018
Magnitude: 6.8

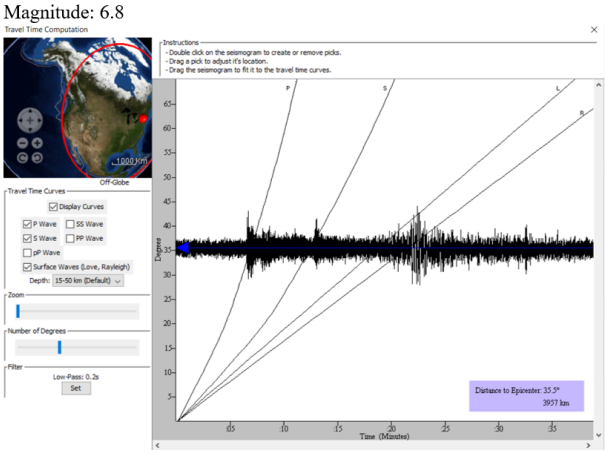

Ithaca High School Seismometer
Event Location: Amarillo, TX, USA
Event Time: 13:04:29 UTC October 20th, 2018
Magnitude: 3.7

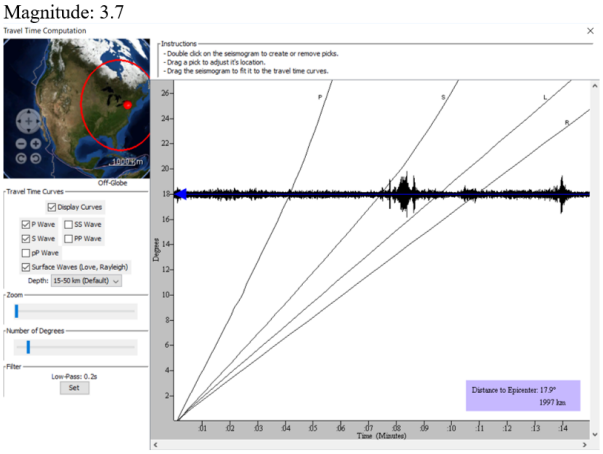

Figure 68: Earthquakes recorded by a broadband sesimometer deployed at Dryden and Ithaca high schools. By identifying the arrival of p-waves, s-waves, and surface waves, the distance between the instrument and the event location can be calculated. The free software Jamaseis, provided by the Incorporated Institutions for Seismology (IRIS), was used to analyze collected data.